VLÁKNA A TEXTIL

FIBRES AND TEXTILES

Volume 33
March
2026

TECHNICAL UNIVERSITY OF LIBEREC

STU FCHPT

Trenčianska univerzita Alexandra Dubčeka v Trenčíne
Fakulta priemyselných technológií v Púchove

VUTCH
RESEARCH INSTITUTE OF TEXTILE CHEMISTRY
VÝSKUMNÝ ÚSTAV TEXTILNEJ CHÉMIE

CHEMOSVIT FIBROCHEM

VÚCHV

ZVTS

Indexed in:
SCOPUS
Chemical Abstract
World Textile Abstracts
EBSCO Essentials

ISSN 1335-0617
print version

ISSN 2585-8890
online version

VLÁKNA A TEXTIL

http://www.vat.ft.tul.cz

PUBLISHED BY
Technical University of Liberec, Faculty of Textile Engineering
Slovak University of Technology in Bratislava, Faculty of Chemical and Food Technology
Alexander Dubček University of Trenčín, Faculty of Industrial Technologies
Slovak Society of Industrial Chemistry, Bratislava
Research Institute of Man-Made Fibres, JSC, Svit
Research Institute of Textile Chemistry (VUTCH) Ltd., Žilina
Chemosvit Fibrochem, JSC, Svit

PUBLISHER
Technical University of Liberec
Studentska 1402/2, 461 17 Liberec 1, CZ
Tel: +420 485 353615
e-mail: vat@tul.cz
IČO: 46747885

ORDER AND ADVERTISEMENT OF THE JOURNAL
Technical University of Liberec
Faculty of Textile Engineering
Studentska 1402/2, 461 17 Liberec 1, CZ
Tel: +420 485 353615
e-mail: vat@tul.cz

TYPESET AND PRINT
Polygrafie TUL, Voroněžská 1329/13, 460 01 Liberec 1, CZ

DATE OF ISSUE
April 2026

APPROVED BY
Rector's Office of Technical University of Liberec
Ref. no. RE 15/26, 6th May 2026

EDITION
First

PUBLICATION NUMBER
55-015-26

PUBLICATION
Quarterly

SUBSCRIPTION
60 EUR

REG. NO. MK ČR E 24338

VLÁKNA A TEXTIL

Volume 33, Issue 1, April 2026

CONTENT

MILITARY FABRICS MADE OF HEMP FIBERS

RASTORHUIEVA, MARIIA; BOIKO, HALYNA*; YEVTUSHENKO, VALENTYNA AND ARTEMENKO, MARIIA

Kherson National Technical University

ABSTRACT

The relevance of this research is determined by the necessity to replace the existing camouflage fabrics on the Ukrainian market, which are made with synthetic fibers for military clothing, with eco-friendly fabrics produced from natural raw materials – hemp fiber. The aim was to analyze the qualitative properties of mixed hemp fabrics developed by scientists of Kherson National Technical University and to determine their potential use in military uniforms. Comprehensive methods of analysis, synthesis, observation, measurement, comparison, and generalization of results were applied, as well as standard methodologies widely used in the light industry. The paper provides a detailed analysis of the current state of the global protective and military textile market. Samples of existing camouflage fabrics for military uniforms and equipment were examined, and results of testing new hemp fiber-based fabrics were presented. Physico-mechanical, aesthetic, and operational tests demonstrated that hemp-based materials surpass most existing analogs in their qualitative characteristics. The introduction of hemp fabrics into military textile production may ensure increased reliability, functionality, and environmental safety of defense products.

KEYWORDS

Assortment, Camouflage Fabrics, Comparative Analysis, Mixed Hemp Fabrics, Properties, Purpose.

INTRODUCTION

In the context of Russia's full-scale invasion, Ukraine's need for high-quality, functional, and safe military textile materials has become critically important. Providing service members with advanced fabrics is not merely a matter of comfort or protection but a strategic factor directly influencing the nation’s defense capability. Modern warfare is characterized by rapidly changing conditions, elevated risks, and the necessity to adapt military gear to extreme climatic, physical, and tactical loads.

Traditional synthetic materials used in military uniforms possess several significant drawbacks: high production costs, considerable energy consumption, limited environmental performance, and potential adverse health effects for personnel. These materials do not always ensure adequate comfort across Ukraine's diverse climatic zones, and prolonged wear may lead to skin irritation and allergic reactions [1]. Under such circumstances, the search for alternative fibrous resources with improved hygienic, ecological, and operational properties becomes particularly relevant.

Ukraine possesses substantial fibrous potential—namely hemp fibers, which have been historically cultivated in the country and are once again demonstrating high technological and economic promise. Hemp fibers exhibit high tensile strength, abrasion resistance, hygroscopicity, inherent bactericidal properties, and environmental purity [2]. These characteristics make them a promising raw material for the development of advanced military textiles capable of ensuring comfort, protection, and durability under demanding operational conditions. The use of domestic natural resources would also strengthen the national textile industry and reduce dependence on imported raw materials.

Global trends indicate the dynamic development of innovations in military textile materials—from nanotechnologies to bioactive, bacteriostatic, and ultra-high-molecular systems [3-7]. Improvement of such materials aims to enhance ballistic protection, reduce equipment weight, improve camouflage performance, and increase the physical resilience of military personnel. For Ukraine, which remains engaged in prolonged warfare, integrating these technologies into the production of natural, environmentally safe, and competitive hemp-based textiles represents a strategically significant direction.

Thus, the relevance of the study lies in the need to develop innovative, eco-friendly, and high-performance military textile materials using Ukraine's own fibrous resources. This will improve the effectiveness and safety of service members and enhance the country's defense-industrial capacity under conditions of armed aggression.

* **Corresponding author:** Boiko H., e-mail: galina_boyko_86@ukr.net

Received October 17, 2025; accepted March 6, 2026

LIBRARY STRUCTURE

Contemporary research in military textiles is focused on developing high-performance materials capable of providing comprehensive protection for service members across a wide range of operational environments. The demand for next-generation military fabrics is driven by increasingly stringent requirements for wear resistance, durability, camouflage performance, moisture resistance, contamination resistance, and stability against microorganisms, chemicals, and mechanical stressors. For this reason, researchers are actively engaged in improving artificial and synthetic fibers while also investigating natural components, particularly bast fibers.

Among natural fibers, hemp has attracted special scientific interest owing to its advantageous performance properties, which make it suitable for use in technical and, specifically, military textiles. For example, researchers at the U.S. Army Natick Soldier Research, Development and Engineering Center in Natick, Massachusetts, including Quoc T. Truong and Natalie Pomerantz [8], are working on enhancing the performance of military textiles through the application of omniphobic coatings. Such coatings improve garment durability, enable self-cleaning behavior, and provide protection against moisture as well as hazards encountered during operations in chemically and biologically contaminated environments.

In the study by Jasti A. and co-authors, a comprehensive characterization of elementary hemp fibers and hemp-based fabrics was conducted. The authors demonstrated that hemp possesses high tensile strength, an optimal cellulose content, considerable crystallinity, and a favorable strength-to-weight ratio, making it competitive with conventional synthetic technical fibers [9]. The study also emphasized the excellent hygienic properties of hemp materials, an important factor for military uniforms used across diverse climatic conditions.

A review by Zimniewska M. systematizes current data on the physico-mechanical and technological properties of hemp fibers, including their suitability for processing, spinning, and weaving. The author concluded that hemp is a promising material for eco-textiles and technical fabrics due to its combination of environmental sustainability and functional performance. Compared to cotton or flax, hemp exhibits higher strength, lower shrinkage, and strong resistance to microbial degradation, qualities that are particularly relevant for military applications [10].

Issues of standardization and the lack of unified methodologies for assessing hemp fiber quality are discussed in the review by Kirk H. et al. The authors provide a detailed analysis of different approaches to studying the morphology, structure, and properties of hemp fibers and emphasize the need for harmonized testing methods, which would facilitate broader industrial adoption, including in high-technology sectors such as protective textiles [11]. The review also highlights natural variability among hemp fibers as a key technological challenge that must be addressed through improved primary processing methods.

One promising direction in current research is the modification of hemp fiber structure to enhance spinnability and fiber uniformity. In the study by Rastorhuieva M. et al., the effects of pulsed electric treatment on the cottonization process of hemp fibers were examined. The results showed that electric-pulse treatment improves fiber flexibility, reduces stiffness, and enhances fiber fibrillation, all of which are crucial for obtaining stable spinning blends and fabrics with superior mechanical properties [12]. This approach opens new opportunities for large-scale use of hemp fibers in the production of specialized textiles.

According to V.M. Durach and L.G. Nikolaychuk [13], the production of apparel for military personnel is a promising segment of the Ukrainian market; however, the performance requirements for such products are exceptionally high. To establish a reliable technological process for manufacturing military uniforms and to supply high-quality products for defense needs, the availability of high-quality natural fabrics preferably made from domestic raw materials is essential.

Given the studies summarized above, hemp fibers demonstrate significant potential for use in military textile production, as they combine high strength, natural hygroscopicity, biological resistance, comfort, environmental sustainability, and the capacity for property modification through modern technological methods. An additional advantage is Ukraine's domestic raw-material base for hemp cultivation, which makes this field strategically beneficial in the context of import substitution and development of the national defense-industrial complex. The use of Ukrainian-grown hemp fibers in next-generation military textiles can ensure independence from external suppliers, reduce production costs, and enhance overall fabric functionality.

MATERIALS AND METHODS

Materials

Nine fabric samples were selected for the study, including seven camouflage materials of different fiber compositions and two blended hemp fabrics with different weave structures. Fabric samples were purchased from various Ukrainian enterprises specializing in the production of military fabrics. The camouflage fabric samples had the following characteristics: sample №. 1 – Rip-Stop "Komfort", khaki color; sample №. 2 – Rip-Stop "Komfort", dark

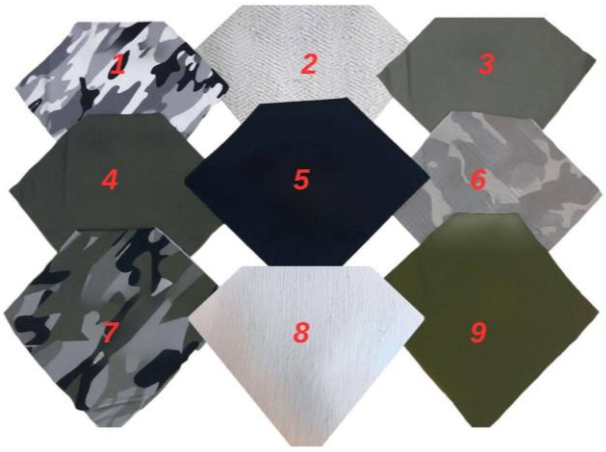

Figure 1. Investigated camouflage fabric samples: Sample №1 – Rip-Stop "Comfort", khaki color; Sample №2 – Rip-Stop "Comfort", dark blue color; Sample №3 – Rip-Stop "TC"; Sample №4 – "Olive"; Sample №5 – "Khaki"; Sample №6 – "Defensa"; Sample №7 – "White Night". Investigated blended hemp fabric samples: Sample №8 – Blended hemp fabric, broken twill weave 2/2; Sample №9 – Blended hemp fabric, plain weave 1/1.

blue; sample №. 3 – Rip-Stop "TC"; sample №. 4 – "Olivka" (olive green); sample №. 5 – "Khaki"; sample №. 6 – "Defensa"; and sample №. 7 – "Bila Nich".

For comparative analysis, two samples of blended hemp fabrics were also included: sample №. 8 featured a broken twill 2/2 weave, while sample № 9 had a plain weave 1/1. The samples were developed by researchers of Kherson National Technical University and manufactured at the Edelvika private joint-stock company, which specializes in the production of linen fabrics. A visual representation of all examined samples is presented in Figure 1.

The selected materials allow for a comprehensive assessment of the physico-mechanical properties of traditional camouflage fabrics alongside newly developed blended hemp fabrics and enable evaluation of their suitability for military applications.

Methods

The investigation of textile materials was carried out in accordance with the requirements of DSTU 21790:2008 "Cotton and Blended Fabrics for Clothing" and DSTU 4057–2001 "Textile Materials. Method for Fiber Identification" (ISO 833:1977) [15]. The research was carried out in the laboratories of Khmelnytskyi National University and the production laboratory of the Edelvika company. The results were based on the average values from ten repeated experiments.

For each tested parameter, measurements were performed on a series of specimens in accordance with the requirements of the relevant standards. Unless otherwise specified by the standard method, not less than five test specimens (n = 5) were used for each fabric property. The values presented in the tables and figures represent the arithmetic mean of repeated measurements. Error bars in the graphical representations indicate the variability of the results and correspond to the standard deviation calculated from the repeated tests.

The purpose of fiber identification was to determine the homogeneity and quantitative composition of the fibrous content. The samples were separated into warp and weft yarns, which were analyzed by combustion to assess odor, burning behavior, and ash residue. Additionally, microscopic examination of the longitudinal and cross-sections of fibers was performed, enabling identification of fiber type, morphological characteristics, and compliance with standards. All analyses were conducted based on the requirements of current normative documentation governing the testing of textile materials [16-25].

The surface density of fabrics was determined by weighing a 10 × 10 cm specimen and recalculating the value per 1 m^2. This parameter characterizes the material's mass and its suitability for different categories of clothing. Warp and weft densities were determined by counting the number of yarns per 50 mm and recalculating the value per 100 mm, providing information on fabric structure and weave uniformity. The linear density (tex) was calculated from the mass and length of the yarn, allowing assessment of yarn thickness and uniformity.

Mechanical properties, tensile strength and elongation, were determined on an RT-250 tensile testing machine under constant extension. The maximum breaking load, absolute elongation, and relative elongation were measured, providing a characterization of fabric strength and deformation behavior.

Crease recovery was assessed using an FG-07 device by measuring the recovery angle after folding and loading. This indicator depends on the elastic properties of fibers and the weave structure and is used to evaluate the fabric's shape retention.

Dimensional stability after laundering was determined to evaluate fabric performance in use. Samples marked with control indicators were subjected to standard washing at 70–80 °C, followed by drying and ironing. Shrinkage was calculated as the percentage reduction in dimensions in both warp and weft directions.

Air permeability was measured on the AT-2 device, recording the amount of air passing through 1 m^2 of fabric in 1 s at a constant pressure drop. The indicator characterizes the comfort and functionality of the material. Water permeability was determined using a special device, which determined the volume of water passing through the sample under a pressure of 200 mm of water. The water permeability coefficient allows you to assess the hydrophilicity and suitability of the fabric for use in wet conditions.

Abrasion resistance was determined on an IT-3M apparatus using an abrasive gray overcoat cloth. The average number of cycles to destruction was recorded, representing the primary criterion for fabric durability.

RESULTS AND DISCUSSION

In global science and industry, an active search continues for new solutions aimed at improving military textiles, particularly materials with enhanced performance characteristics, increased resistance to external influences, and reduced environmental impact. Despite significant progress in innovative textile development, the use of natural bast fibers, particularly hemp, in military fabrics still requires thorough scientific justification and systematic comparison with existing materials. This underscores the need to examine the physico-mechanical properties of hemp-based fabrics to evaluate their suitability for operation under the specific conditions of military use.

Given the increasing requirements for the functionality and reliability of textile materials, it is essential to determine the extent to which hemp fabrics meet the standards applied to materials intended for military applications, and whether they are capable of providing an adequate level of strength, abrasion resistance, air permeability, and dimensional stability. In this context, comparative analysis of natural fibers against traditional synthetic materials, currently dominant in the military sector, becomes particularly relevant.

To address these scientific objectives, a comprehensive study of modern military textile samples was conducted, and their physico-mechanical characteristics were analyzed. Based on the obtained results, and considering the inherent properties of hemp fibers, researchers at Kherson National Technical University developed samples of hemp-based fabric whose functional parameters and application potential are comparable to those of materials traditionally used in the defense industry. The developed sample served as the foundation for further experimental studies and for assessing its potential as an alternative material for military purposes.

The physico-mechanical properties of the fabrics were determined in accordance with standard methodologies outlined in the relevant normative documents [16-20], and the obtained results were compared with the requirements of current standards.

All determinations were carried out in compliance with the relevant ISO and EN standards using the specified number of test specimens for each test method. For linear density, 5–10 yarns were tested in both warp and weft directions. For surface density, thread density, breaking load, elongation at break, abrasion resistance, air permeability, water permeability, dimensional change after wet treatment, and crease resistance, the number of specimens tested was as defined by the corresponding standards. The values recorded in the table are the average results of the measurements (5 yarns). The results of the study regarding the physico-mechanical properties of camouflage fabrics and blended hemp fabrics are presented in Table 1.

The analysis of the physico-mechanical properties of camouflage fabrics made it possible to assess their suitability for various military operating conditions. The samples with a dominant share of hemp fibers (№. 8-9) demonstrated higher tensile strength and abrasion resistance compared to most camouflage samples. This indicates the real potential of hemp-based fabrics as durable raw materials for products exposed to intensive wear. The high thread counts and increased surface density of the hemp samples explain their enhanced mechanical strength and abrasion resistance.

Air permeability ranged from 61.1 to 245.4 $dm^3/m^2 \cdot s$, with sample № 8 exhibiting the best performance. The hemp-based samples showed higher air permeability and water absorption, making them more breathable and comfortable, though less water-resistant. For field conditions, where both moisture protection and ventilation are critical, combined solutions (hemp fabric + hydrophobic coating/membrane) are advisable. The hemp fabrics also demonstrated superior behavior during wet processing (0% shrinkage) and significantly higher crease recovery coefficients. This represents a substantial advantage for military uniforms, ensuring the preservation of garment shape and dimensions during use and maintenance. Furthermore, the hemp samples exhibited considerably higher relative elongation at break, which may indicate increased plasticity, an additional benefit in the manufacture of military apparel.

After wet processing, the smallest deformation was observed in samples № 3 and № 4, while samples № 8 and № 9 maintained their original dimensions entirely, indicating strong dimensional stability after laundering. The highest crease recovery coefficients were recorded for samples № 7 and № 9 (75%), enabling them to retain their shape and appearance after wear.

To visually demonstrate the advantages and limitations of the developed hemp fabrics in comparison with existing camouflage materials, graphs of the most significant properties were prepared, including tensile strength, abrasion resistance, and water permeability (Figs. 2-4).

Hemp fabric samples (№ 8 and № 9) demonstrate the highest breaking load indicators both in the warp and in the weft. Traditional synthetic and cotton samples have lower values, especially in the weft, which emphasizes the superiority of hemp fabrics in strength. Synthetic mixed fabrics (№ 1, № 4) show stable results, but are inferior to hemp in absolute values.

Table 1. Results of the study of physico-mechanical properties of camouflage fabrics and blended hemp fabrics.

Property		Sample								
		1	**2**	**3**	**4**	**5**	**6**	**7**	**8**	**9**
Material composition		30% cotton, 70% polyester	100% cotton	100% cotton	30% cotton, 70% polyester	100% cotton	100% cotton	70% cotton, 30% polyester	70% hemp, 20% cotton, 10% polyester	70% hemp, 20% cotton, 10% polyester
Linear density, [tex]	Warp	25	20	40	25	27	34	33	40	38
	Weft	25	20	33	25	25	38	40	48	46
Surface density, [g/m^2]/ ISO 3801:2019		191	136	211	200	182	187	202	326	314
Threads per 10 cm, [pieces]/ EN 1049-2:2004	Warp	460	530	450	420	580	410	370	642	610
	Weft	230	290	230	240	310	250	280	354	322
Breaking load, [N]/ ISO 5082-82	Warp	765	451	1137	579	902	559	1049	1210	1150
	Weft	255	245	862	470	725	294	490	882	879
Elongation at break, [%]/EN ISO 13984-1:2018	Warp	7.5	7.0	16.5	11.5	10.0	10.0	27.0	24.8	26.7
	Weft	10.0	17.5	16.0	13.0	15.5	13.5	21.0	27.0	28.4
Abrasion resistance to hole formation, [cycles]/ ISO 12947-2:2005		3142	2038	6023	4925	2410	2075	5256	6100	5980
Air permeability, [dm^3/m^2·s]/ ISO 9237:2003		191.7	144.4	61.1	100.0	69.4	208.3	225.0	245.4	220.8
Water permeability, [dm^3/m^2·s]/ EN ISO 811:2018		0.17	0.20	0.22	0.16	0.25	0.18	0.23	0.31	0.28
Dimensional change after wet treatment, [%]/ ISO 5077-2001	Warp	-1.5	-2.5	0	-1.5	-2.0	-1.5	-1.0	0	0
	Weft	0	-1.0	-2.5	0	0	-0.5	-0.5	0	0
Crease resistance, [%]/ISO 5077-2001		35	33	52	21	27	31	75	70	75

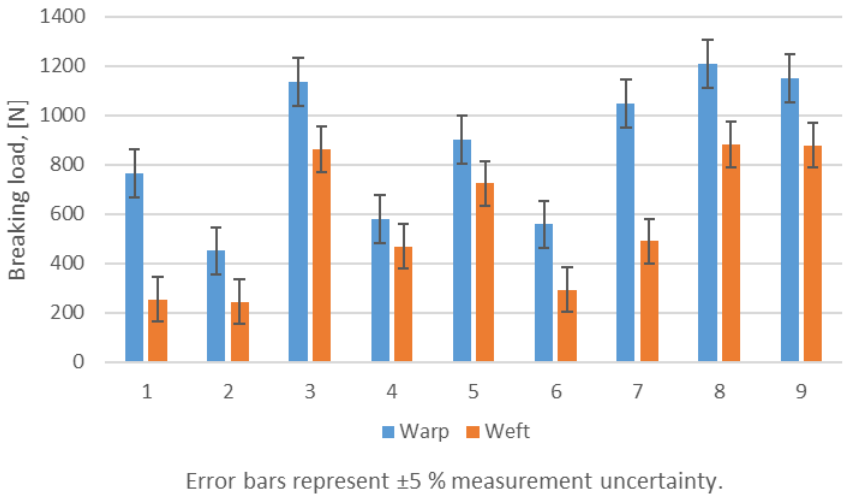

Figure 2. Breaking load of the studied fabric samples (mean ± SD).

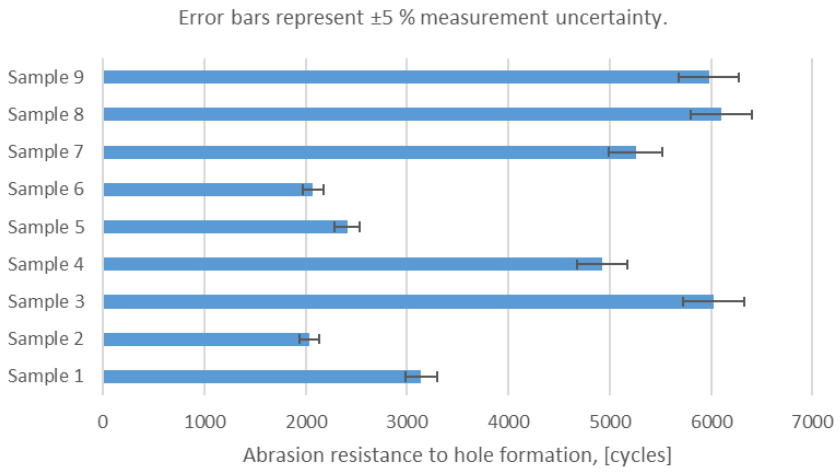

Figure 3. Resistance of the studied fabric samples to wiping (mean ± SD).

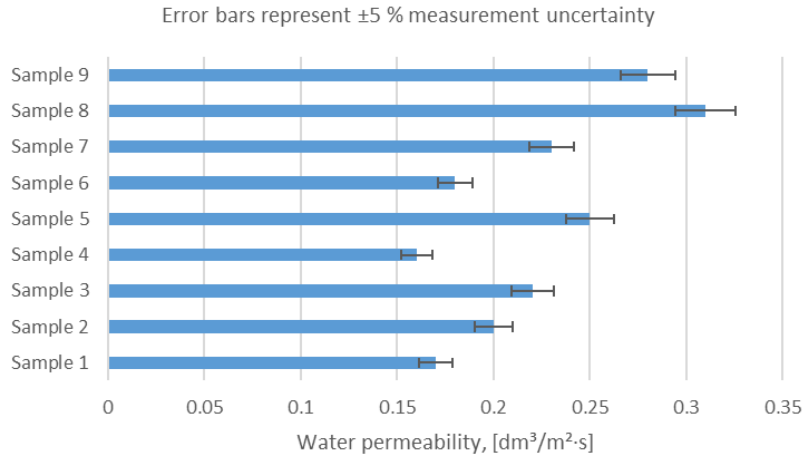

Figure 4. Water permeability of the tested fabric samples before wiping (mean ± SD).

The analysis of resistance to wiping indicated the superiority of samples № 8 (6100 cycles) and № 9 (5980 cycles), which confirms their high wear resistance, the closest to these indicators from camouflage fabrics is № 3, which withstood 6023 cycles.

Water permeability showed minor variations among the samples, with the highest levels observed in samples № 8 and № 9. The water resistance of the blended hemp fabrics is influenced by the chemical composition and microstructure of hemp fibers. According to studies conducted by researchers at Kherson National Technical University [26][27], hemp fibers are covered by a cuticle – a thin layer of waxes and lipids exhibiting hydrophobic properties, which reduces the fiber's ability to absorb water. This layer acts as a natural protective barrier, enabling the fibers to maintain moisture resistance under environmental exposure and preventing excessive water uptake that could lead to structural degradation.

Owing to the combined effect of the hydrophilic nature of cellulose, the primary chemical component of hemp fibers, and the hydrophobic waxy coating on their surface, modified hemp fibers possess balanced hydrophilic-hydrophobic characteristics. As a result, they are capable of absorbing moisture from the environment and maintaining a stable level of humidity without forming large droplets on the surface. This combination makes hemp fibers more resistant to moisture and contamination compared to other natural fibers, such as cotton.

Thus, based on the conducted physico-mechanical studies of camouflage fabric samples and the developed mixed hemp fabric samples, it was determined that samples № 8 and № 9 outperform existing camouflage fabric samples in terms of strength, wear resistance, dimensional stability, elasticity, and water resistance. Additionally, hemp fiber fabrics exhibit high air permeability, which supports oxygen retention within the textile structure, preventing the development of anaerobic bacteria and their proliferation in various types of clothing, footwear, and underwear. The use of such materials not only provides the defense sector with high-quality products but also promotes the use of domestic raw materials.

Further studies were aimed at determining:

- the colorfastness of camouflage fabrics, which defines their durability and scope of application;
- wash fastness, ensuring suitability for everyday and military clothing;
- resistance to distilled water, which is important for textiles used in wet conditions;
- resistance to organic solvents, a necessary requirement for industrial and technical fabrics;
- resistance to dry friction, which affects color retention in areas of intensive contact;
- resistance to ironing, which is important for maintaining the aesthetic appearance of the material.

Assessment of these characteristics allows for determining the compliance of fabrics with operational and functional requirements and estimating their service life.

Since the study investigated mixed hemp fabrics without dyeing or bleaching, these samples were tested for all the aforementioned factors except colorfastness. The evaluation of all camouflage fabric samples for resistance to various environmental and mechanical factors was conducted following the methods outlined in the relevant standards [23][24][25]. The results of the tests are presented in Table 2.

Analysis of the resistance of camouflage fabrics and mixed hemp fabrics showed that all investigated samples exhibit high wash fastness, resistance to distilled water, and resistance to organic solvents (5/5), indicating their durability under various operational conditions.

Resistance to dry friction varied from 3/4 to 5/5, with sample № 5 demonstrating the lowest rating, which may indicate a higher susceptibility to mechanical impact. Other fabrics exhibited stable resistance within the range of 4-5/5, making them suitable for intensive use.

Regarding ironing resistance, all samples except sample № 5 demonstrated the maximum score of 5/5, indicating their ability to maintain shape and structure after thermal treatment.

Overall, all camouflage fabrics and mixed hemp yarn fabrics exhibit excellent operational characteristics, making them promising for use in military clothing of various types. The highest overall resistance was observed in samples № 7 and № 9, whereas sample № 5 requires additional attention regarding friction and ironing resistance.

The conducted studies of physico-mechanical properties and colorfastness indicate that the most suitable samples for clothing production are № 7, № 3, № 8, and № 9. Samples № 7, № 8, and № 9 exhibit high elasticity (ranging from 24.8% to 28.4%), ensuring comfort during wear and ease of movement. These samples also demonstrate the best air permeability, making them suitable for lightweight and breathable garments. Additionally, they have the highest crease recovery coefficients, ensuring the preservation of garment shape even after frequent use and laundering.

Samples № 3, № 8, and № 9 are the strongest and show the highest wear resistance, as confirmed by breaking load values and abrasion cycles, making them ideal for military clothing as well as workwear subjected to intensive mechanical stress.

To determine the aesthetic characteristics of all investigated samples, organoleptic evaluation was performed, assessing the following properties: color, gloss, texture, pattern, touch, and plasticity. Table 3 presents the results of the organoleptic assessment of the aesthetic properties of the camouflage and mixed hemp fabric samples.

According to Table 3, camouflage fabric samples № 1 and № 3, as well as mixed hemp fabric samples № 8 and № 9, are soft, non-prickly, and pleasant to the touch. In contrast, samples № 2, № 4, № 5, and № 6 are stiff, coarse, and slightly prickly, making them unsuitable for the production of undergarments and military underwear. Samples № 1, 2, 4, 5, 8, and № 9 do not exhibit pronounced patterns, ornaments, or a highly textured woven structure. Samples № 3, № 6, and № 7 differ in coloration, which makes them suitable for use in military camouflage clothing. The colors of samples № 8 and № 9 are closer to their natural shades without the use of dyes, making them suitable for eco-friendly footwear and clothing, as well as for summer-season military camouflage apparel. Figure 5 presents a profilogram of the organoleptic evaluation of the aesthetic properties of the investigated camouflage and mixed hemp fabrics intended for military applications.

According to the results of the organoleptic profilogram analysis, several key patterns can be identified:

1. Camouflage fabric samples № 1 and № 3, as well as blended hemp fabrics № 8 and № 9, exhibit softness, smoothness, and pleasant tactile sensations, which makes them suitable for products that come into direct contact with the skin, including underwear and next-to-skin military apparel. Samples № 2, № 4, № 5, and № 6 are characterized by greater stiffness, roughness, and a slight pricking effect. Although these properties limit their use in direct-contact garments, they do not preclude their application in outerwear or technical textile products.
2. Samples № 1, 2, 4, 5, 8, and № 9 possess a uniform texture without pronounced relief or ornamentation, making them suitable for solid-color or camouflage garments where fabric neutrality is required. In contrast, samples № 3, № 6, and № 7 feature varying shades and noticeable surface relief, which enhances their applicability for military camouflage clothing, where the texture supports blending with the natural environment.

Table 2. Resistance of camouflage fabrics and mixed hemp fabrics to various influencing factors, points.

Fabric Name	Property Name				
	Wash Fastness	Resistance to Distilled Water	Resistance to Organic Solvents	Resistance to Dry Friction	Ironing Resistance
Sample №1	5/5	5/5	5/5	4/5	5/5
Sample №2	5/5	5/5	5/5	4-5/5	5/5
Sample №3	5/5	5/5	5/5	4-5/4-5	5/5
Sample №4	5/5	5/5	5/5	4-5/5	5/5
Sample №5	5/5	5/5	4-5/5	3/4	4-5/4-5
Sample №6	5/5	5/5	5/5	4-5/5	5/5
Sample №7	5/5	5/5	5/5	5/5	5/5
Sample №8	5/5	5/5	5/5	4-5/5	5/5
Sample №9	5/5	5/5	5/5	5/5	5/5

Table 3. Organoleptic evaluation of the aesthetic properties of the investigated fabric samples.

Property	Sample1	Sample 2	Sample 3	Sample 4	Sample 5	Sample 6	Sample 7	Sample 8	Sample 9
Color and Shade	Khaki with a grayish tint	Dark blue	Camouflaged coloration with shades from light gray to dark gray	Olive with a dark green tint	Khaki with a light gray tint	Camouflaged coloration with shades from light green to dark green	Camouflaged coloration with shades of white, black, gray, and green	Gray with beige tint	Beige with grayish and brownish tints
Gloss	Matte	Slight, barely noticeable	Silky gloss	Slight, barely noticeable	Silky gloss	Matte	Matte	Silky gloss	Silky gloss
Texture	Smooth, cool, light, pleasant to touch	Dense, rough, coarse, not very pleasant to touch	Fuzzy, embossed, slightly rough	Smooth, warm, pleasant to touch	Smooth, cool, light, pleasant to touch	Smooth, cool, dense, light, pleasant to touch	Fuzzy, rough, not very pleasant to touch	Moderately textured, warm, fluffy	Pleasant to touch, textured, warm, fluffy
Ornament/Pattern	No pattern or ornament, uniform	Textured without patterns or ornaments	Camouflaged pattern, not prominent	Solid, without patterns or ornaments	Solid, structural, without ornaments	Camouflaged pattern with distinct multicolor streaks	Camouflaged pattern with distinct multicolor streaks	No pattern, barely noticeable twill ornament, uniform	Natural structure, no patterns or ornaments
Touch	Soft	Feels dense and firm	Soft	Soft, dense fabric	Firm	Soft, dense	Moderately stiff, firm	Soft	Soft
Plasticity	Slightly plastic	Almost non-plastic	Plastic	Slightly plastic	Moderately plastic	Moderately plastic	Plastic	Well plastic	Well plastic

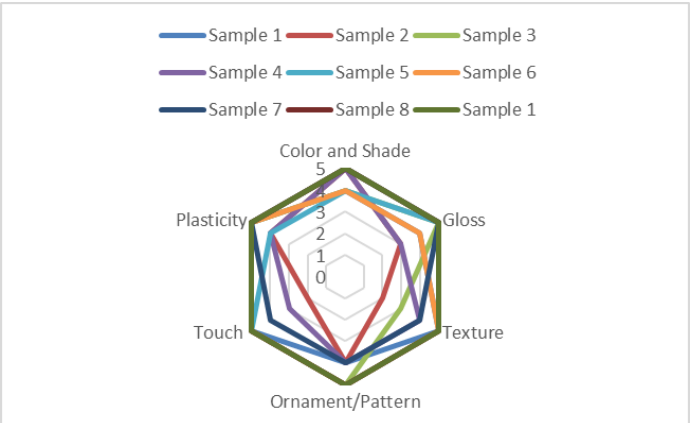

Figure 5. Profilogram of the organoleptic evaluation of the aesthetic properties of camouflage and mixed hemp fabrics.

3. Hemp-based samples № 8 and № 9 demonstrate a natural, unprocessed fiber color without additional dyes. This makes them suitable for environmentally oriented products, including lightweight camouflage clothing and footwear, that meet the requirements for environmental resistance and reduced chemical impact.

The profilogram clearly demonstrates that blended hemp fabrics № 8 and № 9 combine pleasant tactile properties, natural coloration, and sufficient surface versatility, making them the most promising materials for next-to-skin, camouflage, and eco-oriented military textile applications. Camouflage fabric samples № 3, № 6, and № 7, owing to their relief and tonal variation, are more appropriate for outer camouflage garments.

CONCLUSION

The conducted studies encompassed the analysis of physico-mechanical, operational, and aesthetic properties of commercially available military camouflage fabrics, as well as experimental samples developed from mixed hemp yarn. The results indicated that while traditional synthetic and blended materials exhibit satisfactory characteristics, they are outperformed by the new hemp-based samples in several key parameters. Specifically, hemp fabrics show increased tensile and abrasion strength, improved vapor and air permeability, high hygroscopicity, and resistance to biological factors.

Comprehensive evaluation demonstrated that the use of hemp fabrics not only provides a higher level of operational reliability but also enhances wearing comfort, which is especially important under military service conditions. Therefore, hemp fabrics can be considered more promising for use in the production of military clothing, footwear, and underwear, supporting the rationale for their further implementation in military textiles.

Studies of the resistance of camouflage and hemp fabrics to various external factors, such as washing, friction, organic solvents, and ironing, determine their durability and suitability for operational conditions.

The high color stability of camouflage fabrics ensures the preservation of both camouflage functionality and aesthetic qualities, which is critical for military apparel. Hemp fabrics, due to their natural beige-gray-green shades, can be used to produce garments with protective coloration without the need for dyes. This makes them practical for military and specialized applications in sandy or desert environments, as the material is simultaneously eco-friendly, durable, and naturally camouflaging.

The research confirmed the importance of further development of military fabrics made from mixed hemp yarn, their adaptation to modern military needs, technical textiles, and military equipment. Advancing production technologies and analytical methods will allow for optimization of material properties, ensuring effectiveness, durability, and environmental safety.

REFERENCES

1. Boyko G.A., Prokopchuk V.V.: Analysis of the properties of bast raw materials as a component of fabric for military uniforms, Tovaroznavny visnyk. Lutsk, 17(1), pp. 9-17, 2024. https://doi.org/10.62763/ef/1.2024
2. Boyko G., Holovenko T., Yageluk S., et al.: Methods for improving the qualitative indicators of fabric on the basis of hemp cotonine for the top of footwear, Fibres and Textiles, 28(2), pp. 3-8, 2021. http://vat.ft.tul.cz/2021/2/VaT_2021_2_1.pdf
3. Pimenta C., Fangueiro R., Morais C.: Thermal Camouflage Clothing in Diurnal and Nocturnal Environments, Key Engineering Materials, 893, pp. 37-43, 2021. https://doi.org/10.4028/www.scientific.net/KEM.893.37
4. Lim T., Jeong S.M., Seo K., et al.: Development of fiber-based active thermal infrared camouflage textile, Appl. Mater. Today, pp. 20-28, 2020. https://doi.org/10.1016/j.apmt.2020.100624
5. Steffens F., Gralha S.E., Ferreira L.L.S., et al.: Oliveira Military Textiles – An Overview of New Developments, Key Engineering Materials, Trans Tech Publications Ltd, Switzerland, 812, pp. 120-126, 2019. https://doi.org/10.4028/www.scientific.net/KEM.812.120
6. Loghin C., Ciobanu L., Lonesi D., et al.: Introduction to waterproof and water repellent textiles, Waterproof and Water Repellent Textiles and Clothing, The Textile Institute Book Series, 17, pp. 3-24, 2018. https://doi.org/10.1016/B978-0-08-101212-3.00001-0
7. Shuvo I.I., Dolez P.I.: Design of a military protective suit against biological agents, Functional and Technical Textiles, The Textile Institute Book Series, pp. 141-176, 2023. https://doi.org/10.1016/B978-0-323-91593-9.00009-2
8. Truong Q.T., Pomerantz N.: Military applications: Development of superomniphobic coatings, textiles and surfaces, Waterproof and Water Repellent Textiles and Clothing, The Textile Institute Book Series, p. 473-531, 2018. https://doi.org/10.1016/B978-0-08-101212-3.00016-2
9. Jasti A., et al.: Characterization of Elementary Industrial Hemp Fiber and Woven Fabric for Potential Applications in Technical Textiles, Journal of Natural Fibers, pp. 580–596, 2022. https://doi.org/10.1080/15440478.2022.2158982
10. Zimniewska M.: Hemp Fibre Properties and Processing Targeted to Textile: A Review, Materials, 15(5), pp. 1901, 2022. https://doi.org/10.3390/ma15051901
11. Kirk H., et al.: A Critical Review of Characterization Methods for Textile Hemp Fibre, Cellulose, 30(14), pp. 8595–8616, 2023. https://doi.org/10.1007/s10570-023-05420-4
12. Rastorhuieva M., et al.: Effect of Electric Pulse Treatment on Cottonization of Hemp Fiber, Fibres & Textiles in Eastern Europe, 32(2), pp. 82–89, 2024. https://doi.org/10.15240/tul/008/2024-2-002
13. Durach V.M., Nikolaychuk L.H.: Directions for improving special clothing for servicemen of the Armed Forces of Ukraine to enhance their safety. Formation and prospects of entrepreneurial structures development within the framework of European integration: Proceedings of the 4th International Scientific and Practical Conference, Poltava: State Agrarian University, pp. 100–102, 2021. https://doi.org/10.36477/2522-1221-2022-31-05
14. DSTU 4057-2001: Textile materials. Fiber identification method. Effective from 2002-05-01. Official edition. Kyiv: State Standard of Ukraine, pp. 33, 2002.
15. ISO 7211-5:2020: Textiles — Methods for analysis of woven fabrics construction — Part 5: Determination of linear density of yarn removed from fabric. https://cdn.standards.iteh.ai/samples/74893/e7fc3637301b4e0bbc668705ff8cf92d/ISO-7211-5-2020.pdf
16. SIST EN 12127:1999: Textiles - Fabrics - Determination of

mass per unit area using small samples 12127:1999. https://cdn.standards.iteh.ai/samples/11546/35670d3f3f1b44839c28e18cd094de4b/SIST-EN-12127-1999.pdf
17. ISO 7211-5:2020: Textiles — Methods for analysis of woven fabrics construction Part 5: Definition linear density yarn removed from fabric 7211-5:2020. https://www.iso.org/ru/standard/74893.html
18. ISO 9073-3:2023: Nonwovens — Test methods Part 3: Determination of tensile strength and elongation at break using the strip method. https://www.iso.org/ru/standard/83591.html
19. ISO 12947-2:2016: Textiles — Determination of the abrasion resistance of fabrics by the Martindale method — Part 2: Determination of specimen breakdown. https://cdn.standards.iteh.ai/samples/61058/3a51b7cddceb4708bc7ea9c900c6cdc4/ISO-12947-2-2016.pdf
20. ISO 9237:1995: Textiles — Determination of the permeability of fabrics to air. https://www.iso.org/ru/standard/16869.html
21. DSTU ISO 9865-2001: Textile materials. Determination of water resistance of fabrics by sprinkling according to the Bundesmann method. Effective from 2002-01-01. Official edition. Kyiv: State Enterprise "UkrNDNTs", pp.10, 2002.
22. ISO 9865:1991: Textiles — Determination of water repellency of fabrics by the Bundersmann rain-shower test. https://cdn.standards.iteh.ai/samples/17742/a9205e94ce85421a9561cbad3cc89f52/ISO-9865-1991.pdf
23. ISO 105-C06:2010: Textiles — Tests for colour fastness Part C06: Colour fastness to domestic and commercial laundering. https://www.iso.org/standard/51276.html
24. EN ISO 105-E01:2010: Textiles — Tests for colour fastness Part E01: Colour fastness to water. https://www.iso.org/standard/52230.html
25. ISO 105-X12:2001: Textiles — Tests for colour fastness Part X12: Colour fastness to rubbing. https://www.iso.org/standard/32339.html
26. Boiko H.A., Berezovsky Y.V., Rakityanska V.V.: Influence of the anatomical structure of technical hemp fibers on the hydrophobic properties of footwear products based on them, Bulletin of Lviv University of Trade and Economics, 31, pp. 7–13, 2022.
27. Yaheliuk S., Fomich M.: Optimizing fuel rolls from crop residues using comprehensive quality indicator (CQI), Engineering for Rural DevelopmentOpen source preview, 24, pp. 491–496, 2025. https://doi.org/10.22616/ERDev.2025.24.TF106

PERCOLATION-GOVERNED FORMATION OF CONDUCTIVE NETWORKS IN POLYANILINE-FUNCTIONALIZED TEXTILE COMPOSITES

REDKO, YANA[1*] AND HUDZENKO, NATALIIA[2]

[1] Kyiv National University of Technologies & Design, Mala Shyianovska (Nemyrovycha-Danchenka) srt. 2, 01011 Kyiv, Ukraine
[2] Leibniz Institute for Composite Materials GmbH, Erwin-Schrödinger-Str. 58, 67663 Kaiserslautern, Germany

ABSTRACT

Conductive polyaniline (PANI)-based textiles are developed using a heterocoagulation-controlled deposition mechanism. In contrast to conventional in situ polymerization, this approach exploits the interaction between oppositely charged PANI particles and textile substrates to form specialized percolation networks. Polyamide substrates form highly interconnected networks with excellent conductivity, while cotton nonwovens exhibit less regular pathways. The heterocoagulation approach allows for fine-tuning of the layer structure, lowers the percolation threshold, achieves high conductivity while maintaining textile flexibility, and enhances durability against washing, dry, and wet rubbing. This methodology presents a systematic approach for controlling the structure–property–percolation relationship in conductive textiles, enabling potential applications in sensors, antistatic fabrics, and flexible electronics.

KEYWORDS

Polyaniline; Heterocoagulation; Electrically conductive textiles; Percolation networks; Textile materials; Surfactant-assisted deposition.

INTRODUCTION

Surface modification of textile fibers is widely used to tailor their functional properties and expand the application potential of textile materials. Previous studies have demonstrated that modification of polyacrylonitrile fibers and polyamide textile substrates can significantly influence their surface characteristics and functional performance [1] [2]. Such approaches enable the development of advanced textile materials with enhanced electrical and physicochemical properties. Among various strategies, the formation of electrically conductive networks in polymer-modified textiles has attracted increasing attention for applications in antistatic materials, sensors, and flexible electronic systems.

Conducting polymers, particularly polyaniline (PANI), have attracted considerable interest in the textile industry due to their light weight, flexibility, tunable electrical properties, and potential for wearable electronics [3–9]. Traditionally, PANI has been deposited onto textile substrates by in situ polymerization or simple coating methods, achieving moderate conductivity. However, existing methods often fail to control the formation of continuous conductive networks on fiber surfaces, resulting in limited reproducibility, high percolation thresholds, and mechanical instability [3–6]. In particular, in situ polymerization methods do not fully exploit the role of particle-substrate interactions or the influence of surface charge on percolation network formation [10]. An alternative approach involves surface deposition mechanisms, where conductive polymer particles or nuclei are selectively assembled on textile fibers through interfacial interactions. In particular, heterocoagulation, based on the electrostatic attraction between oppositely charged particles and substrates, offers a promising avenue for directing the organization of the conductive phase on the fiber surface [11–13].

The key concept underlying charge transport in heterogeneous conducting systems is the percolation theory, which describes the transition from an insulating to a conducting state after reaching a critical concentration of conducting domains [14] [15]. Beyond the percolation threshold, the appearance of percolation networks – continuous, interconnected structures spanning the volume of the material, provides long-distance electron transport. In textile composites, the formation of such networks is strongly influenced by the structural and raw material composition, the nature of the fiber surface, spatial confinement, and the method of deposition of the conductive phase [16] [17]. Therefore, controlling the

[*] **Corresponding author:** Redko Y., e-mail: 82yanet@gmail.com
Received January 23, 2026; accepted March, 18, 2026

formation of the percolation network remains a central problem yet it is rarely addressed explicitly in terms of deposition mechanism–driven network topology in textile systems in the development of electrically functional textile materials. Thus, the aim of the work is to determine how the heterocoagulation-controlled deposition of PANI on textile substrates of different raw material composition and structure affects the formation of percolation networks and the electrical conductivity of the material. This will allow establishing structure–property–percolation relationships to ensure optimal electrical conductivity with a minimum content of active conductive polyaniline.

To achieve this aim, the following objectives were defined:

1. To synthesize electrically conductive textile materials by depositing polyaniline onto polyamide knitted fabrics and cotton nonwoven substrates under surfactant-assisted heterocoagulation conditions.
2. To evaluate the effect of anionic surfactants on polyaniline deposition efficiency and electrical conductivity, in comparison with systems synthesized without surfactants.
3. To analyze electrical conductivity as a function of aniline concentration, identifying percolation thresholds and conductivity transitions for different textile substrates.
4. To compare percolation behavior in structurally ordered (polyamide knitted) and disordered (cotton nonwoven) textile systems, highlighting the influence of fiber structure on conductive pathway formation.
5. To establish structure–property–percolation relationships, demonstrating that electrical conductivity is governed primarily by the formation and connectivity of percolation networks rather than by the total amount of deposited polyaniline.

EXPERIMENTAL

Polyamide (PA) continuous filament yarn with a linear density of 15.6 tex was used as the base material. A knitted polyamide fabric produced from this yarn was employed as one textile substrate. A cotton nonwoven material was used as a second substrate for comparison.

Conductive textile materials were prepared by oxidative polymerization of aniline directly in the treatment bath in the presence of textile substrates and surfactants. Aniline oxidation was carried out using ammonium peroxydisulfate as an oxidizing agent. The molar ratio of oxidizer to aniline was maintained at 1:1.3. An anionic surfactant, sulfonol (sodium alkylbenzenesulfonate, ASAS), was used to control particle charge and deposition behavior.

The treatment process was performed at a bath temperature of 18–22 °C with a treatment time of 15–30 min. Under these conditions, nanodispersed polyaniline particles were formed in situ and deposited onto the textile substrates through a heterocoagulation mechanism, driven by electrostatic attraction between oppositely charged particles and fiber surfaces [18]. After treatment, the conductive textile samples were thoroughly rinsed with distilled water and dried under ambient conditions.

The electrical resistance of the treated textile materials was measured using a two-electrode compensating method, which allows determination of both bulk and surface resistance (R) with an ohmmeter. Electrical resistance measurements were performed at several locations on each textile sample in order to account for the inherent structural heterogeneity of textile materials. For each experimental condition, multiple measurements were carried out and the reported values correspond to the average results. The variability of the measurements is expressed as standard deviation (±SD). Electrical conductivity (σ) was calculated from the measured resistance values.

Color fastness of the conductive textile materials was evaluated according to standard test methods: washing fastness (DSTU ISO 105-S06:2009), perspiration fastness (DSTU ISO 105-E04:2009), and dry and wet rubbing fastness (DSTU ISO 105-X12:2009).

The amount of polyaniline deposited on the textile substrates was assessed indirectly by measuring the optical density (D) of the treated samples dissolved in sulfuric acid. The optical density was assumed to be proportional to the polyaniline content, and, consequently, to the initial aniline concentration in the treatment bath.

RESULTS AND DISCUSSION

In this study, a controlled heterocoagulation deposition mechanism was applied to deposit polyaniline (PANI) onto textile substrates. The approach is based on electrostatic attraction between oppositely charged PANI particles and textile fibers in the presence of anionic surfactants. Polyamide knitted fabrics and cotton nonwoven materials were selected as model substrates to evaluate the influence of fiber surface charge, substrate structure, surfactant concentration, and aniline content on conductive network formation and percolation behavior.

Effect of surfactants on polyaniline deposition

During aniline oxidation in the treatment bath, the use of ionic and nonionic surfactants allows the formation of colloidal dispersions of emeraldine salt with different surface charges. For heterocoagulation-controlled deposition, both the sign and magnitude of the ξ-potential of PANI particles and the textile surface are crucial.

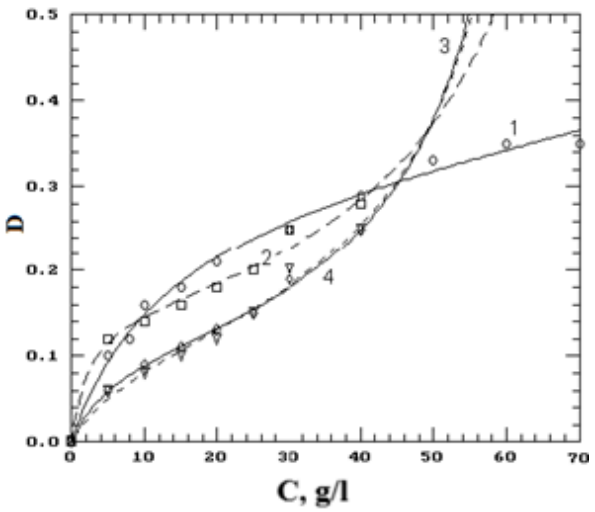

Figure 1. Dependence of optical density (D) of TM-treated solutions on aniline concentration (C): 1 – without surfactant; 2 – 0.5 g/l ASAS; 3 – 1 g/l ASAS and 4 – 2 g/l ASAS.

Table 1. Effect of aniline and surfactant concentration in the treatment bath on the synthesis of polyaniline on PA textile material.

C ASAS, [g/l]	Equation type*	Empirical equation parameters
0	$S = 0{,}01;$ $R = 0{,}997$ $y = \frac{a+bx}{1+cx+dx^2}$	$a = 0.00268;$ $b = 0.02392$ $c = 0.066;$ $d = -0.0002$
0.5	$S = 0.013;$ $R = 0.99$ $y = \frac{a+bx}{1+cx+dx^2}$	$a = 0.00028;$ $b = 0.0689$ $c = 0.429;$ $d = -0.0053$
1	$S = 0.012;$ $R = 0.993$ $y = \frac{a+bx}{1+cx+dx^2}$	$a = 0.00318;$ $b = 0.01246$ $c = 0.0698;$ $d = -0.0011$
2	$S = 0.006;$ $R = 0.998$ $y = \frac{a+bx}{1+cx+dx^2}$	$a = 0.00036;$ $b = 0.0189$ $c = 0.1349;$ $d = -0.0021$

* S – standard deviation; R – correlation coefficient; x – aniline concentration in the bath in g/l; y – optical density.

Polyamide fibers in acidic media (pH below the isoelectric point, pH < 5) exhibit a positive surface charge due to protonation of amino groups. When an anionic surfactant (sodium alkylbenzene sulfonate, ASAS) is used, PANI particles acquire a negative surface charge. This charge combination enables classical heterocoagulation, where negatively charged PANI particles are adsorbed onto the positively charged polyamide surface [19].

Surfactant molecules adsorbed on the surface of insoluble PANI particles suppress their uncontrolled growth and reduce particle–particle coagulation. As a result, the dispersion remains stable, and particle deposition onto fibers becomes more uniform.

Polyaniline content and sorption behavior

Figure 1 shows the dependence of the amount of synthesized PANI on the aniline concentration and surfactant content in the treatment bath. The experimental data are well described by empirical equations with correlation coefficients ranging from 0.99 to 0.998 (Table 1).

In the absence of surfactants (curve 1, Fig. 1), the dependence exhibits a typical sorption behavior with a tendency toward saturation. This behavior is characteristic of conventional dyeing processes, where dye uptake is limited by adsorption or absorption mechanisms [20] [21].

In contrast, in the presence of anionic surfactants, the shape of the curves changes qualitatively. A sharp increase in optical density is observed at aniline concentrations above 35–40 g/L, and no clear saturation is detected. Since PANI solutions in sulfuric acid obey the Bouguer–Lambert–Beer law, the optical density is directly proportional to the amount of deposited conductive polymer. Therefore, the observed behavior indicates a change in the deposition mechanism rather than simple sorption.

Applicability of the Langmuir model

Since polyaniline solutions in sulfuric acid obey the Bouguer-Lambert-Baer law, the optical density of solutions of dyed textile materials in sulfuric acid is proportional to the amount of electrically conductive dye (polyaniline) on the textile material. In the presence of anionic surfactants, the nature of the dependence undergoes a qualitative change: the curves do not show a tendency to saturation, but there is a rather sharp increase in optical density with an increase in the aniline concentration above 35 – 40 g / l. Thus, it can be stated that in the presence of anionic surfactants, the nature of the dye sorption changes qualitatively.

The curve of the dependence of the amount of synthesized dye on the aniline concentration in the absence of surfactants (curve 1 in Fig. 1) is a conventional dye sorption curve, which is characterized by a tendency to saturation. Knowledge of the process mechanism allows us to develop methods for intensification of dyeing processes. With a linear dependence of the dye concentration in the fiber on the dye concentration in the bath, the process of dye dissolution in the textile is usually taken as the mechanism, with a nonlinear isotherm, as a rule, the adsorption of the dye molecule on some internal surface of the fiber is taken as the mechanism [20] [21].

The nonlinear dye sorption isotherm can be described by the Langmuir model, which assumes adsorption

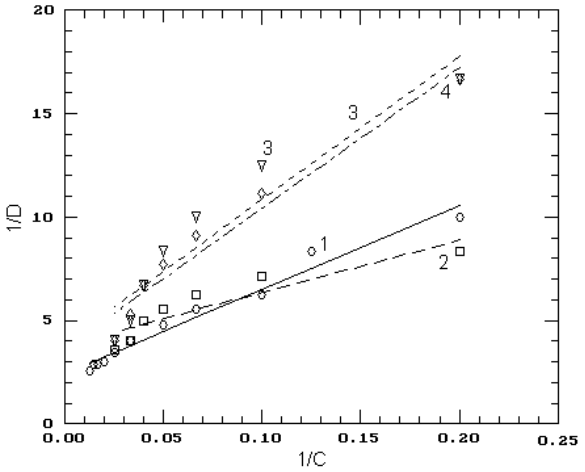

Figure 2. Dependence of the optical density of TM-treated solutions on the aniline concentration in the coordinates of the Langmuir equation. 1 – without surfactant; 2 – 0.5 g/l surfactant; 3 – 1 g/l surfactant and 4 – 2 g/l surfactant.

Table 2. Parameters of lines in Langmuir equation coordinates.

SAS Content [g/l]	$a \pm \sigma_a$	$b \pm \sigma_b$	*R*
0	40.7 ± 2.3	2.42 ± 0.18	0.99
0.5	25 ± 5	3.8 ± 0.5	0.91
1	70 ± 10	3.9 ± 0.9	0.95
2	68 ± 6	3.6 ± 0.5	0.98

with the formation of a monomolecular layer on the fiber surface. This approach has been successfully applied in previous studies on disperse dye sorption [22] demonstrating its adequacy for describing adsorption processes in textile materials. In the present study, the Langmuir equation is used in its linearized form [20] [21]:

$$\frac{1}{C_f} = \frac{1}{C_{f,\infty}} \frac{1}{KC_{f,\infty}} \cdot \frac{1}{C_S} \quad (1)$$

$C_{F,\infty}$ – saturation value corresponding to the filling of the monomolecular layer; K – sorption-desorption equilibrium constant, C_F i C_S – concentration of dye in the fiber and in the external environment at equilibrium.

The analysis of the dye dissolution process in the fiber under the assumption that the solvate theory of solutions can be applied was carried out in [20]. As active centers, fragments of macromolecules with an energy of intermolecular interaction sufficient for the formation of solvates were taken. The interaction of active centers with plasticizer molecules dissolved in an amorphous polymer takes into account the rule of molar particles [21]. When a low-molecular compound is sorbed by a polymer due to adsorption or absorption (with the formation of solvates) of intermolecular interactions, which provide the "lifetime" of the sorbate molecule in the adsorption layer or in the solvate similarly. For the absorption process with the formation of solvates, the expression [19] was obtained [20]:

$$\frac{1}{C_f} = B + A\frac{1}{C_S} \quad (2)$$

were $A = 1/(K_D + KC_{FMC,\infty})$ and $B = K/(K_D + KC_{FMC,\infty})$, K_D – dye distribution coefficient, $K = K_{MC}K_D$, K_{MC} – equilibrium constant in the reverse process of dye solvate formation, $C_{FMM,\infty}$ – maximum possible concentration of active centers.

Comparison of equations (1) and (2) shows that for the description of the absorption of a dye in a textile material, an equation similar in form to the Langmuir equation for monomolecular adsorption of a dye can be obtained. As can be seen from Fig. 2, the Langmuir equation coordinates describe the synthesis of polyaniline on a textile material in the absence of surfactant additives quite well. An objective assessment of the degree of adequacy of the description of the experimental data by a straight line in the coordinates of the Langmuir equation is possible using the least squares method.

For samples of polyamide textile material, in the absence of anionic surfactant in the dye bath, the dependence of the optical density (D) of the solution of the fabric dyed with a polymer dye on the concentration of aniline in the dye bath (C) is described by a straight line with a correlation coefficient of 0.986 (3):

$$1/D = (2.42 \pm 0.18) + (40.7 \pm 2.3)(1/C) \quad (3)$$

When deriving the Langmuir equation, it was assumed that dye molecules are adsorbed from the solution in the form of a monomolecular layer [20, 21]. During processing, aniline in the solution is in three states: a saturated solution in water, a solution in micelles due to solubilization, and dispersed aniline. When studying the real processing process, the total concentration of aniline in the processing bath was used, which does not correspond to the initial assumptions of the Langmuir equation. In this case, linearity in the coordinates of the Langmuir equation is the linearity of a parabola given in the reciprocals of the argument and the function. A similar type of functional dependence is characteristic of reversible processes with saturation [20]. Thus, the nature of the dye absorption isotherm curve by the fiber cannot be used as a criterion for the mechanism of dye-fiber interaction (dissolution or adsorption). To establish the mechanism of sorption of aniline or its oxidation products, it is necessary to use methods that are not related to the Langmuir equation.

Comparison of the standard deviations of the parameters of the straight lines in the coordinates of the Langmuir equation (Fig. 2) shows (Table 2) that the nature of the synthesis process, reflected in its result, is different for processing baths without and with the content of surfactants. It should be noted that the main changes occur at a surfactant concentration of up to 1 g/l, the dependence of the optical density on the concentration of aniline in the processing bath

are practically identical (Fig. 1, Table 2) at surfactant concentrations in the range of 1–2 g/l. Thus, comparison of the standard deviations of the parameters of the straight lines shows that the nature of the sorption of polyaniline particles is different for processing baths without and with the content of surfactants (Table 2). Therefore, the nature of the sorption isotherm curve cannot be a criterion for the interaction of polyaniline with PA TM (dissolution or adsorption of molecules from the solution in the form of a monomolecular layer).

A possible reason for the qualitative difference in the nature of the process of synthesis and sorption of polyaniline by fiber may be the process of heterocoagulation of negatively charged colloidal particles of polyaniline (due to the sorption of surfactant anions on their surface) on the positively charged surface of the polyamide fabric (at a pH greater than the isoelectric point, the surface of the polyamide textile material is positively charged due to the ionization of amino groups).

Electrical conductivity and percolation behavior

Polyaniline belongs to the class of electronically conductive polymers [12] [23]. They can be considered as derivatives of a polymer whose base form has the structure (a) and consists of reduced (b) and oxidized (c) repeating units (Fig. 3).

Complete protonation of the nitrogen atom in the imino group in the emeraldine base by an aqueous solution of hydrochloric acid (doping) is accompanied by a sharp increase in electrical conductivity [12] [23].

The first percolation threshold is the concentration of the electrically conductive component (in this case, the emeraldine salt), above (or at) which a continuous chain of particles of the conductive component appears. The sample loses its insulator properties and becomes a conductor, although the electrical conductivity may be significantly lower than that of metals.

Due to the structural heterogeneity of textile materials, electrical resistance was measured at several locations on each sample, and the reported conductivity values represent the average of repeated measurements. The standard deviation of the measurements did not exceed 8–12%, confirming acceptable reproducibility of the obtained data.

Figure 4 shows the dependence of electrical conductivity on aniline concentration for polyamide knitted fabrics and cotton nonwoven materials. For both substrates, the use of anionic surfactants leads to a significant increase in conductivity, with differences reaching up to two orders of magnitude compared to systems synthesized without surfactants.

A pronounced decrease in conductivity is observed in the aniline concentration range of 5–10 g/L. In composite systems containing a conductive phase dispersed in an insulating matrix, such behavior is typically associated with disruption or incomplete formation of percolation networks [14]. Once the first percolation threshold is exceeded, a continuous conductive pathway is formed, and the material transitions from an insulating to a conductive state.

Influence of substrate structure and surfactant on percolation network formation

The textile structure strongly affects percolation network formation. Polyamide knitted fabrics exhibit lower percolation thresholds and higher conductivity due to their ordered fiber arrangement and stable inter-fiber contacts. These features facilitate the formation of interconnected conductive pathways.

It should be noted that the selected substrates differ not only in fiber chemistry but also in structural organization. Polyamide knitted fabrics represent a structurally ordered textile system with relatively stable inter-fiber contacts, whereas cotton nonwoven materials are characterized by a more disordered fiber arrangement and higher structural heterogeneity. Therefore, the observed differences in electrical behavior reflect the combined influence of fiber surface properties and textile morphology on the formation of conductive percolation networks.

In contrast, cotton nonwoven materials show higher percolation thresholds and lower conductivity. Their random fiber orientation and looser structure hinder the formation of continuous networks, requiring higher amounts of deposited PANI to achieve electrical connectivity.

Polyamide knitted fabrics, with their ordered fiber structure, formed well-connected PANI networks, resulting in higher conductivity, while cotton nonwoven substrates, with disordered fibers, exhibited less regular networks and lower conductivity. Comparisons across surfactant concentrations demonstrated that the formation and connectivity of percolation networks, rather than the total polyaniline content, dictate the electrical performance.

Electrical conductivity measurements further confirmed this: samples synthesized with anionic surfactants reached conductivities up to two orders of magnitude higher than those without, even when the total PANI amount was similar. This highlights the critical role of network structure in controlling macroscopic electrical properties.

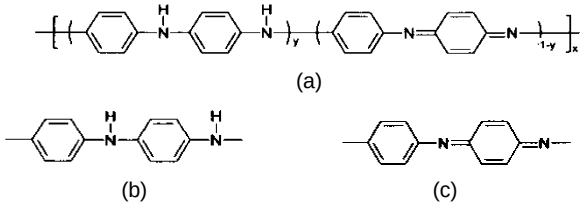

(a) (b) (c)

Figure 3. Structure of polyaniline and its forms.

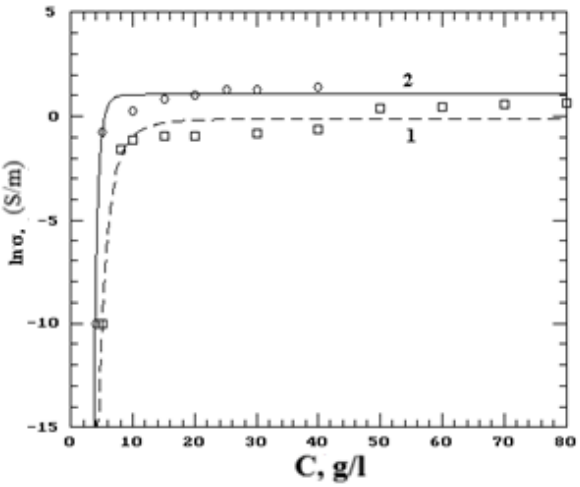

(a)

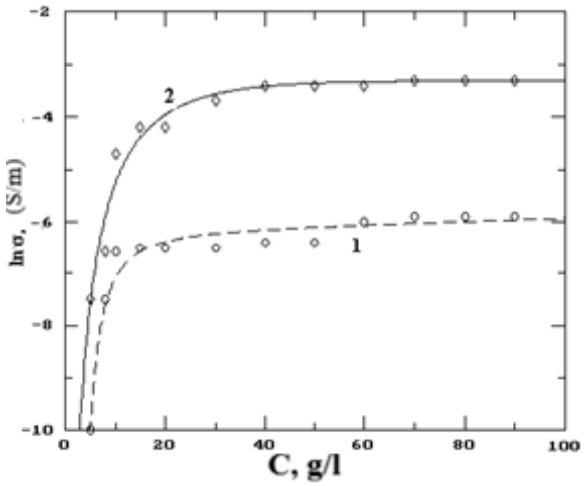

(b)

Figure 4. Dependence of the electrical conductivity of polyamide TM (a) and cotton nonwovens (b) (σ) on the concentration of aniline (C) in the treatment bath. Curve 1 – synthesis without surfactant, curve 2 – synthesis of PANi with 0.5 g/l of surfactant. The presented conductivity values correspond to mean values obtained from repeated measurements on different areas of the textile samples (±SD).

Table 3. Functional properties of the developed electrically conductive of polyamide knitted fabric.

Property	Value
Electrical conductivity σ (S/m)	$(1.0 \pm 0.2) \times 10^{-2}$ – $(1.0 \pm 0.1) \times 10^{2}$
Washing fastness (ISO 105-S06)	5
Rubbing fastness – dry (ISO 105-X12)	4–5
Rubbing fastness – wet (ISO 105-X12)	4–5

* Electrical conductivity values represent mean results obtained from repeated measurements at several locations on the textile samples (±SD).

Overall, these findings show a clear structure–property–percolation relationship: by controlling deposition conditions and fiber interactions, it is possible to optimize conductive network formation and achieve high conductivity at lower polymer content, while preserving textile handle and durability.

The presence of anionic surfactants changed the nature of polyaniline deposition. Optical density measurements showed a sharp increase in polyaniline uptake above 35–40 g/l aniline in the bath, indicating that surfactants not only stabilize particles but also promote network connectivity. The Langmuir model confirmed that sorption alone cannot explain the differences; instead, controlled particle assembly and percolation network formation govern conductivity.

Role of controlled heterocoagulation

Controlled heterocoagulation plays a key role in determining the morphology and connectivity of the conductive phase. Electrostatic attraction between positively charged fibers and negatively charged PANI particles prevents uncontrolled aggregation and promotes uniform particle distribution.

This method allowed precise control of the formation of continuous percolation networks, linking substrate morphology, particle stabilization, and network connectivity to macroscopic conductivity.

Macroscopic conductivity is governed primarily by the formation of continuous percolation networks rather than by the total PANI content. Anionic surfactants perform a dual function: they stabilize PANI particles in the dispersion and direct their adsorption onto fiber surfaces. This leads to improved reproducibility, enhanced conductivity, and better mechanical stability of the conductive layers.The experimental results confirm the initial hypothesis regarding the influence of particle surface charge on PANI deposition during semi-continuous textile treatment. Since polyamide knitted fabric demonstrated significantly higher electrical conductivity after polyaniline deposition compared to the cotton nonwoven substrate, further evaluation of functional durability properties, such as abrasion and washing resistance, was performed only for this textile material (Table 3).

The proposed controlled heterocoagulation deposition mechanism enables the production of electrically conductive textile materials with high washing fastness and abrasion resistance (Table 3), making them promising for smart textiles, sensors, antistatic fabrics, and flexible electronics.

CONCLUSIONS

This study demonstrates that the electrical performance of polyaniline-based textile composites is governed primarily by the formation and connectivity of percolation networks, rather than by the total polymer content. Heterocoagulation-assisted deposition, mediated by anionic surfactants, enables selective assembly of negatively charged PANI particles onto positively charged fiber surfaces, promoting uniform coverage and network connectivity. Comparative analysis of polyamide knitted fabrics and cotton nonwoven materials shows that substrate

structure and surface charge critically influence network formation, percolation onset, and achievable conductivity. Surfactant-assisted heterocoagulation significantly reduces the percolation threshold, allowing high conductivity at lower monomer concentrations while maintaining textile flexibility and handle. These results establish a clear structure–property–percolation relationship, providing practical guidelines for designing electrically conductive textiles with controlled microstructure and optimized functional performance. This framework can support the development of wearable electronics, sensors, smart textiles, and other applications requiring efficient conductive networks.

REFERENCES

1. Garanina O., Panasyuk L., Romaniuk L., et al.: Influence of superficial modification on electrical conductivity of polyacrylonitril fiber. Vlakna A Textil, 2020, 27(2), pp. 49–53. https://vat.ft.tul.cz/Archive/VaT_2020_2.pdf
2. Red'ko Ya.V., Suprun N.P.: XRD and SEM analysis of iron oxide nanoparticles formation in polyamide textile material. Vlakna A Textil, 2018, 25(3), pp. 63–67. https://vat.ft.tul.cz/Archive/VaT_2018_3.pdf
3. Safdar F., Ashraf M., Javid A., et al.: Polymeric textile-based electromagnetic interference shielding materials, their synthesis, mechanism and applications – A review. Journal of Industrial Textiles. 2022, 51(5_suppl), 7293S–7358S. https://doi.org/10.1177/15280837211037085
4. Dhawan S.K., Gupta B., et al.: Shielding effectiveness of conducting polyaniline coated fabrics at 101 GHz. Synth. Metals, 2001, 125, pp. 389–393. https://doi.org/10.1016/S0379-6779(01)00478-7
5. Zhang Y., Dong A., Wang Q., et al.: Conductive cotton prepared by polyaniline in situ polymerization using laccase. Applied Biochemistry and Biotechnology, 2014, 174, pp. 820–831. https://doi.org/10.1007/s12010-014-1094-9
6. Aizamddin M.F., Mahat M.M.: Enhancing the washing durability and electrical longevity of conductive polyaniline-grafted polyester fabrics. ACS Omega, 2023, 8(41), pp. 37936–37947. https://doi.org/10.1021/acsomega.3c03377
7. Mocioiu A.M., Murgulescu O.C.: Conductive textile coated with polyaniline. Proceedings, 2020, 57(1), 95 P. https://doi.org/10.3390/proceedings2020057095
8. Zhang W., Wang X., Li Y., et al.: Recent research advances in textile based flexible power supplies and displays for smart wearable applications. ACS Applied Electronic Materials, 2024, 6(8), pp. 5429–5455. https://doi.org/10.1021/acsaelm.4c00606
9. Stoppa M., Chiolerio A.: Wearable electronics and smart textiles: A critical review. Sensors, 2014, 14(7), pp. 11957–11992. https://doi.org/10.3390/s140711957
10. Tseghai G.B., Malengier B., Fante K.A., et al.: Integration of conductive materials with textile structures: An overview. Sensors, 2020, 20(23), 6910 P. https://doi.org/10.3390/s20236910
11. Olad A., Ilghami F., Nosrati R.: Surfactant assisted synthesis of polyaniline nanofibres without shaking and stirring: effect of conditions on morphology and conductivity. Chem Pap. 2012, 66(8), pp. 757–764. https://doi.org/10.2478/s11696-012-0197-4
12. Birdi K.S. editor. Colloid Stability and Coagulation. In: Handbook of Surface and Colloid Chemistry. 4th ed. Boca Raton, FL: CRC Press; 2015. p. 123–145. eBook ISBN: 9780429169779. https://doi.org/10.1201/b18633
13. Cao H., Zhang L., Wu L., et al.: Characterization of heterocoagulation with oppositely charged polymer colloid particles. ACS Applied Materials & Interfaces, 2016, 8(42), pp. 29136–29147. https://doi.org/10.1021/acsami.6b08916
14. Stauffer D., Aharony A.: Introduction to Percolation Theory. Taylor & Francis, London, 2003.
15. Sahimi M.: Applications of Percolation Theory. Taylor & Francis, 1994, 276 P. https://doi.org/10.1201/9781482272444
16. Andrzej K., Katarzyna K.: Electrical percolation in composites of conducting polymers and dielectrics. Journal of Polymer Engineering, 2015, 35(8), pp. 731–741. https://doi.org/10.1515/polyeng-2014-0206
17. Cherenack K., van Pieterson L.: Smart textiles: Challenges and opportunities. J. Appl. Phys., 2012, 112, 091301 P. https://doi.org/10.1063/1.4742728
18. Suprun N., Red'ko V.: Flexible textile absorbers of electromagnetic radiation. In: Proceedings of the 2019 3rd International Conference on Advanced Information and Communications Technologies (AICT), 2019, pp. 88–91. https://doi.org/10.1109/AICT.2019.8847750
19. Colloidal Particles at Liquid Interfaces. Eds. B. P. Binks and T. S. Horozov. Cambridge : Cambridge University Press, 2006. 503 P.
20. Romankevich O.V.: Absorption isotherm during the formation of sorbat e-polymer solvates. Dopovidi of the National Academy of Sciences of Ukraine, 2006, No. 4, pp.148–151. https://doi.org/10.24127/hj.v13i2.11309
21. Odian G.: Principles of Polymerization. – John Wiley & Sons, 2004, 848 P.
22. Redko Y.V., Romankevich O.V.: Adsorption isotherm of a disperse dye, Journal of Fibre Chemistry, 2006, 38(2), pp. 155–157. https://doi.org/10.1007/s10692-006-0062-8
23. Stejskal J., Gilbert R.G.: Polyaniline. Preparation of a conducting polymer. Pure Appl. Chem., 2002, Vol. 74 (5), pp. 857−867. https://doi.org/10.1351/pac200274050857

MAGNETISABLE MELT-SPUN FIBRES PRODUCED AS LIQUID-CORE HOLLOW FIBRES: DEVELOPMENT OF FIBRES AND EFFECTS OF MAGNETISABILITY

KÖLSCH, LENA; SCHNOCK, OLIVER; FISCHER, HOLGER* AND MAY, DAVID

Faserinstitut Bremen e.V., FIBRE, Bremen, Germany

ABSTRACT

Magnetisable fibres, among others, can be used for targeted fibre arrangement or fixing by use of a magnetic fields, antistatic properties or shielding against electromagnetic fields. In some cases the application requires to keep the functional, magnetic component separate from the environment. Liquid-filled hollow fibres are a promising candidate for this purpose, as the fibre hull material can be chosen to keep optimal interaction with the surrounding environment, while the liquid-phase allows for introduction of large fractions of fillers. In this study, a novel strategy to achieve magnetisable fibres was investigated. By melt spinning, hollow polyethylene fibres were produced and in situ filled with a liquid containing iron oxide particles. As reference, polypropylene monofilaments were melt spun, where the iron oxide particles were compounded into the polymer prior to melt spinning. Both processes were successfully implemented, however in the first strategy the ferrofluid caused deficient process robustness due to nozzle clogging and thermal instability. For rough access of the achievable magnetisability, hollow fibres were filled manually with a ferrofluid. To evaluate magnetic functionality, a custom-built measurement unit was developed for quantifying the magnetic attraction force of fibre samples. The measured magnetic detachment forces of the ferrofluid-filled samples were 17.0 ±0.8 mN and therefore in the range of the monofilaments, where values from 11.4 ±0.7 mN to 26.6 ±1.8 mN were measured, depending on fibre diameter and iron content.

KEYWORDS

Melt spinning; Hollow fibre; Low-pressure filling; Magnetisable fibres; Magnetisability measurement.

INTRODUCTION

Liquid-filled hollow fibres are a promising candidate to introduce special functionalities into textile products, where the functional component is kept separate from the environment within the fibre core. This way, the fibre hull material can be chosen to keep optimal interaction with the surrounding environment. This opens a wide range of possible future applications. Examples are:

- Magnetisable fibres consisting of a thermoplastic hull and oil in the core, containing iron particles [1]. These can be used for applications like fibre arrangement or fixing by use of a magnetic field, creation of materials with antistatic or magnetic properties, shielding against electromagnetic fields etc [2]. Furthermore, iron containing fluids are known for changing their viscosity in magnetic fields [3]. This opens new options for textile sensors or special protective textiles.
- Materials for drug release in medical applications, where slow diffusion through the fibre wall guarantees a long-term release of the active component [4].
- Fibres with immobilized bacteria in the core for e.g. treatment of sewage water, where the fibre hull allows diffusion of the component to be removed by bacterial metabolism into the fibre core [5].
- Shock-absorbing fibres for protective cloth [6], where the energy absorption is realised by the surface friction between the polymer hull and liquid core.

For all these examples liquid-filled hollow fibres potentially give benefits, with the difference in applications requiring either long fibres (just cut after production) or fibres in lengths comparable to classic staple fibres. In any case it is necessary to close the fibre ends to keep the functional liquid separated from the environment.

In general, liquid-filled hollow fibres can be generated using two different pathways. The first of them consists of two steps: first production of hollow fibres and processing them into a textile or composite and subsequently filling the fibres with liquid [7]. For filling

* **Corresponding author:** Fischer H., e-mail: *Fischer@Faserinstitut.de*

Received March 9, 2026; accepted April 9, 2026

there are different options, all of them possible at room temperature: passively using the capillary effect, or by pumping systems either applying pressure [8] or vacuum [7] [9] to soak the liquid into the fibres. Main advantage of these methods is, that there is no demand on temperature stability of the liquid. This enables e.g. filling of glass fibres (produced at high temperatures) but is combined with the disadvantage of limited fillable fibre length (depending on viscosity, internal diameter, surface tension etc.) [10].

The second pathway was developed at EMPA using a special spinneret, where the liquid is injected continuously into the hollow fibre under high pressure. Crucial parameters of this process, influencing the diameters of fibre core and hull, are the ratio between throughput of molten polymer to liquid and their viscosities [11]. Main advantages of this type of process are the unlimited fibre length and high process speeds as base for economical processing [12].

One particular disadvantage of this process is the necessity of applying high pressure to the liquid, preventing e.g. the pumping of liquids containing living bacteria. For this reason, for the works presented in [5], a modified low-pressure pumping system has been successfully introduced into the process, which is the basis for the study at hand.

This article describes the development of the process to generate hollow fibres in-situ filled with an oil containing iron particles ('ferrofluid') by use of a low-pressure system. There is no established method for assessing the magnetisability of individual fibres commercially available. Thus, a custom-built setup for quantifying the magnetic detachment force of the fibres was developed and used in this work.

For comparison and to benchmark the magnetic performance of the liquid-filled fibres, a reference system based on solid composite fibres was required. For this purpose, polypropylene monofilament fibres with iron oxide particles were produced using established polymer fibre manufacturing techniques, which is a proven technology. The typical approach involves integrating magnetic particles – most commonly iron oxides (Fe_3O_4, γ-Fe_2O_3), carbonyl iron, or ferrite powders – into thermoplastic polymers such as polypropylene, polyamide, or polyester prior to extrusion [13-17]. Particle loadings in such fibres typically range from a few percent up to 30 wt%, depending on the desired magnetic response and the constraints imposed by melt viscosity and fibre spinnability [18-20]. These composite fibres have been investigated for various applications including electromagnetic shielding, antistatic textiles, and sensor systems [14-16, 21-29]. Following this established approach, polypropylene monofilament fibres containing iron oxide particles were produced in this study, providing a reference system with well-defined iron content.

MATERIALS AND METHODS

Materials

For the liquid filled hollow fibres, low-density polyethylene (LDPE, LE9168, Borealis, AT with MFR 65 g/10min) was used as sheath material, while refined soybean oil (Chemiekontor, DE, Art. No. 1391-4.5) was used as liquid core. The oil's viscosity is approx. 4.5 mPa·s [30]. Iron oxide particles (Bayoxide® E 8706, Lanxess, DE, average size 30 nm) were mixed in the oil without any additional treatment.

For the monofilaments, polypropylene (PP, Moplen HP561 R, LyondellBasell, NL with MFR 25 g/10 min) was used as fibre and the iron oxide particles were directly compounded in the PP prior to melt spinning.

Methods

Melt-spinning of liquid-filled hollow fibres

Liquid-filled hollow fibres were produced using a modified melt-spinning process with pressureless filling of the fibre core. This enables safely processing of liquids, which are sensitive to pressure changes, i.e. preventing in case of iron particles undesired agglomeration. The key feature of the set-up is a spinneret design in which the polymer melt and the liquid core component remain separated until the spinneret outlet, enabling a merging length of zero. The spinneret (cf. Figure 1) exhibits 18 holes, each with 1.4 mm diameter and internal capillary of 0.8 mm outside diameter and 0.55 mm internal diameter. Subsequently, after leaving the spinneret both components merge, allowing the liquid to be fed without pressure. This approach facilitates the integration of sensitive liquids into the fibre core, which makes it particularly interesting for particle-filled liquids, where the particles could be thermally or mechanically damaged.

A schematic of the process including the applied temperature profile is shown in Figure 2. The polymer (LDPE) was melted in a twin-screw extruder (Leistritz ZSE18) at a screw speed of 100 rpm and conveyed by a gear pump to the spinneret. The extruder zones were operated at temperatures between 110 °C and 130 °C, with a spinneret temperature of 130 °C (see Figure 3). The liquid was transported separately from a reservoir by a peristaltic pump and guided to the centre of each spinneret orifice through coaxially inserted capillaries. At the spinneret outlet, polymer and liquid converged to form liquid-filled fibres, which were subsequently drawn, stretched, and wound. For processing, a spin finish suitable for polyolefins (DURON® OF 4066, Schill+Seilacher, DE) was applied as a 10 wt% solution in distilled water. Multifilament yarns consisting of 18 filaments were obtained at a winding speed of 100 m/min.

Figure 1. Spinneret outlet in detail view during production of liquid filled hollow fibres.

Compounding and melt-spinning of magnetisable polypropylene fibres

Prior to processing, the iron oxide powder was dried for 24 h at 80 °C. Polymer and particles were then pre-mixed before feeding into the extruder. Compounding was carried out on a co-rotating twin-screw extruder (Leistritz, DE) equipped with a 3.5 mm die. The extruder operated at a screw speed of 200 rpm and zone temperatures between 70 °C (feed) and 220 °C (die). The extrusion profile included 13 heating zones, gradually increasing from 70 °C at the feed zone to 220 °C at the die. Compounds with particle loadings of 20 and 30 wt% were produced at a total mass throughput of 2.5 kg/h.

The compounded granules were pelletised and subsequently processed into monocomponent fibres on a melt-spinning line (Fourné Maschinenbau GmbH, Alfter-Impekoven, DE). Fibres were produced at a throughput of 2.1 kg/h and a spin pump speed of 30 rpm.

Optical microscopy

The characterisation of fibre geometry was carried out by light microscopy (Leica MC 120 HD, Leica Microsystems, DE) of fibre cross-sections at randomly selected positions along the multifilaments. For sample preparation, fibres were fixed in a microtome (Figure 4) and cut perpendicular to the fibre axis. The resulting cross-section planes were subsequently examined under bright-field conditions, and outer and inner diameters as well as wall thicknesses were determined from the micrographs.

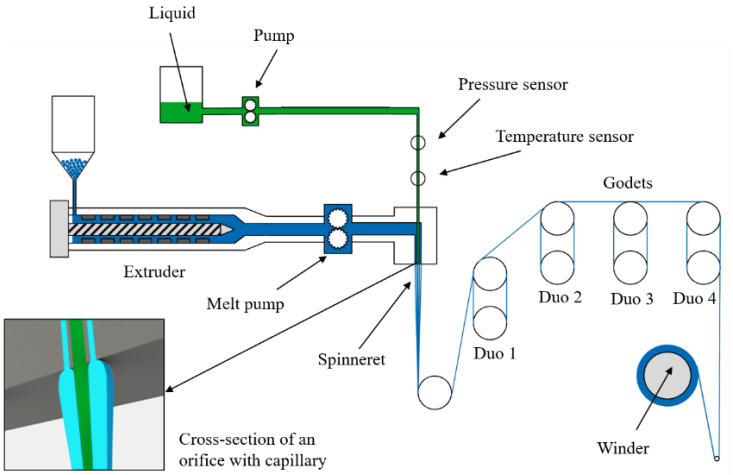

Figure 2. Schematic set-up of the modified melt-spinning process for liquid-filled hollow fibres. The polymer is melted in the extruder and conveyed via a gear pump to the spinneret, while the liquid is transported separately through a hose pump. Polymer melt and liquid core remain separated until the spinneret outlet and only merge after extrusion, enabling pressureless filling of the fibre core.

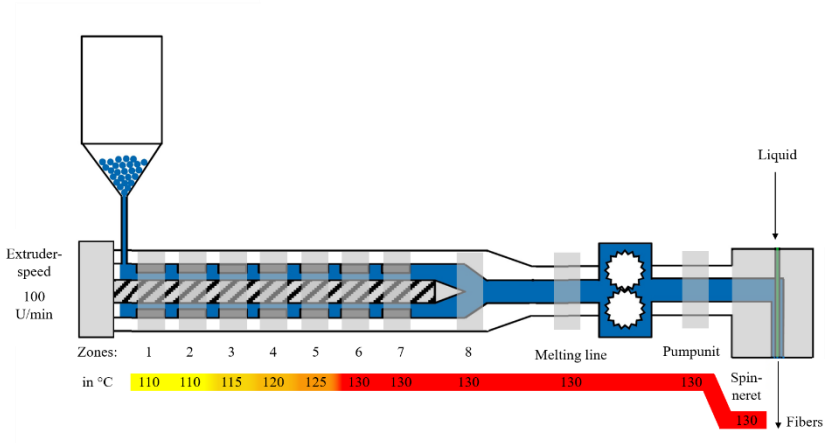

Figure 3. Temperature profile of the extruder used for fibre production. The polymer melt was processed at zone temperatures between 110 °C and 130 °C, with a constant spinneret temperature of 130 °C.

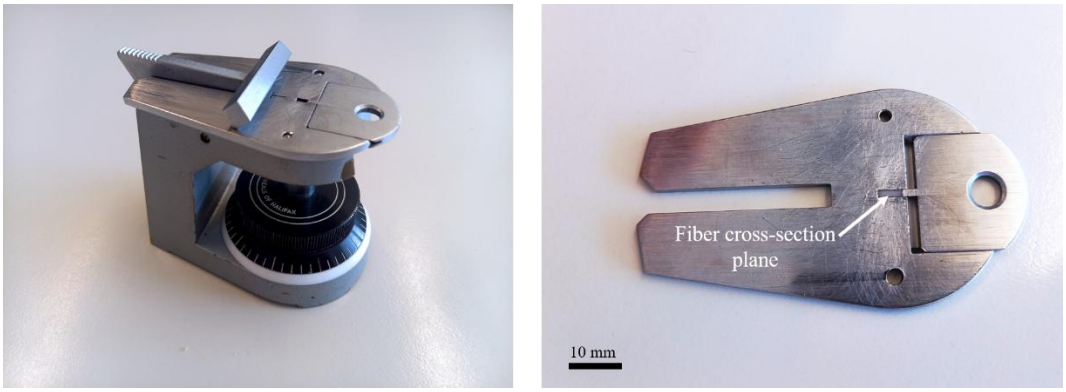

Figure 4. Microtome used for the preparation of fibre cross-sections. Left: microtome device with clamping unit for fibre fixation. Right: positioning of the fibre segment and definition of the cross-section plane obtained for optical microscopy.

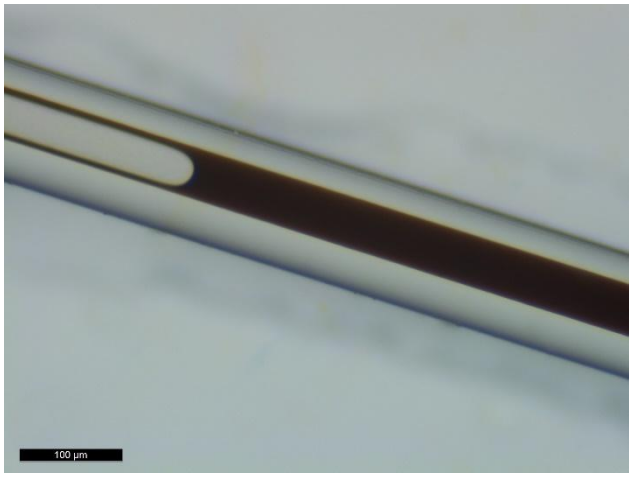

Figure 5. Optical micrograph of the manually liquid-filled hollow fibre.

Magnetisable hollow fibres

LDPE Hollow fibres with diameters of 112 ± 2,3 µm outside and 50 ± 3,1 µm inside were manually filled with a commercial ferrofluid (Laborladen.de, Donaueschingen, DE, Art. No. L10.0071.01000) by capillary forces (cf. Figure 5). This approach was chosen since direct spinning of oil with dispersed iron particles was not stable due to sedimentation and nozzle clogging (see Results section). No quantitative information on the iron content of the ferrofluid was available; the effective iron content of the fibres can be estimated by comparing the results of magnetic detachment to the polypropylene-based compound fibres. This method was suitable to produce enough samples for the magnetic detachment test.

Magnetic characterisation (custom test rig)

In order to quantify the magnetic adhesion force of the fibres, a dedicated test rig was developed (Figure 6). The set-up consists of a glass-fibre reinforced plastic (GFRP) plate on which the fibre bundles are fixed. The plate is equipped with a screw at the bottom side, allowing the specimen to be mounted directly onto a calibrated load cell (KD45 10N, ME-Meßsysteme GmbH, Henningsdorf, DE, Art. No. 14). For all tests, a cable of 36 single filaments single filament was manually wound 40 times around the GFRP plate, ensuring the same number of 1440 filament windings in total for each sample. The tension of manual winding was kept as low as possible to exclude filament elongation. A permanent magnet of 5 mm diameter with an attached string is placed onto the fibre specimen, the sensor is zeroed, and the string is slowly pulled vertically upwards manually by means of a hand crank. The pulling speed was approx. 0.5 mm/s. The force is continuously recorded (sampling rate: 10.64 Hz). The maximum force corresponds to the magnet detachment and is identified by using the @MAX() function in MS Excel. This value is taken as the characteristic magnetic adhesion force. A typical force–time curve is shown in Figure 7. The measurement shows the continuous increase in force as the magnet is lifted, followed by a distinct peak at the point of detachment, which represents the adhesion force. Each measurement was repeated multiple times per fibre type to ensure reproducibility. The load cell is a bending-beam sensor with deformations in the sub-micrometer range, i.e. outside any optically detectable displacement. The measurement therefore directly records the detachment force (peak force), and no displacement information is physically available or relevant for this method. It has to be mentioned, that the measured forces depend directly on magnetic strength and geometry of the permanent magnet used in the set-up. This has to be considered for future developments of this method.

RESULTS & DISCUSSION

Melt-spinning of liquid-filled hollow fibres

Hollow fibres with a liquid core of refined soybean oil were successfully produced using the low-pressure melt-spinning process described above. Figure 8 (left) shows optical micrographs of the resulting multifilaments. The fibres exhibited a homogeneous and continuous liquid core along the filament axis. The outer and inner diameters were uniform over the filament length, and no defects such as ruptures of the fibre wall or leakage of the liquid were observed. The wall thicknesses measured by optical microscopy

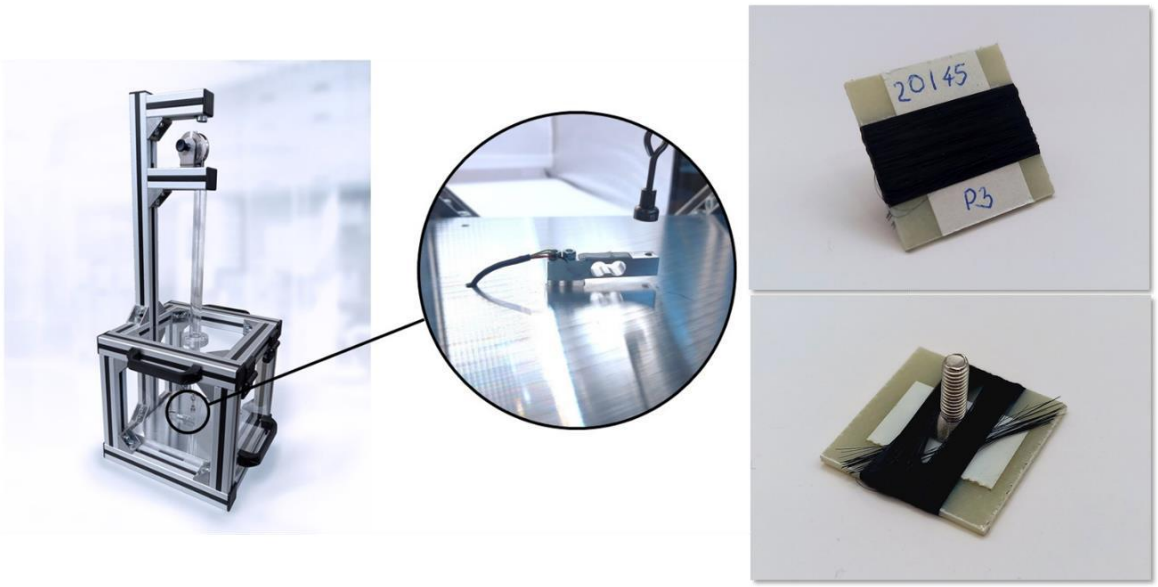

Figure 6. Custom-built test rig for the measurement of magnetic adhesion forces of fibres. Left: overall view of the set-up with vertical frame and integrated load cell. Right: examples of prepared specimens fixed on sample holders for testing (top: fibre bundle, bottom: fibre strands with magnet placed on top, sample size: 15 mm x 15 mm).

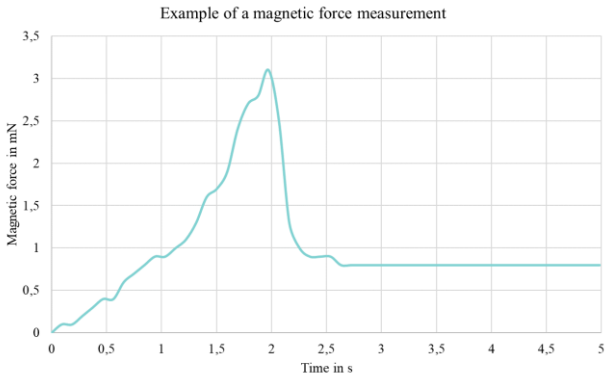

Figure 7. Example of a force–time curve recorded during magnetic adhesion testing. The peak value corresponds to the detachment force of the magnet, which was used as the characteristic adhesion force.

corresponded well to the targeted process parameters, confirming stable processing conditions. The results demonstrate that the low-pressure melt-spinning approach could be transferred in principle, but further development will be necessary for processing magnetisable, particle-containing liquids. Fibres filled with pure soybean oil exhibited continuous, homogeneous cores and stable process conditions, confirming that the liquid dosing system allows reliable core filling without excessive pressure or thermal degradation of the polymer melt.

When the liquid core was replaced by an oil containing dispersed iron oxide particles, the process initially appeared stable, and fibres with a particle-filled liquid core could be produced. However, after short processing time, sedimentation and thermal degradation of the iron-containing liquid occurred, leading to partial clogging of the spinneret and finally to process instability. Moreover, the optical micrographs of these fibres revealed that the particle–oil mixture inside the fibres was not homogeneous. Distinct particle agglomerates (Figure 8, right) can be observed along the fibre axis, indicating that the suspension stability was insufficient under the thermal and shear conditions of the melt-spinning process. The relatively high density and magnetic interaction of the particles likely accelerated sedimentation, while the elevated spinneret temperature promoted changes in viscosity. Similar to observations of Roure & Cunha [31], local concentration gradients occurred, causing clogging of individual capillaries and interruption of the melt flow. Consequently, only short (approximately 10 -15 mm) fibre segments could be obtained.

These findings underline the sensitivity of liquid-core spinning to the rheological and thermal stability of the injected liquid. To achieve stable processing of magnetisable systems, a balance between viscosity, density, and magnetic interaction must be maintained to prevent sedimentation and phase separation. The results further suggest that for applications requiring magnetic functionality, embedding the particles directly in a thermoplastic matrix offers a more robust and scalable approach than dispersing them in a liquid carrier.

Compounding and melt-spinning of magnetisable polypropylene fibres

Magnetisable monofilament fibres with solid particle loading could be produced in a stable and reproducible manner. Both compounds, with 20 wt% and 30 wt% filler loading, showed uniform particle distribution. The magnetisable character of the compounds was immediately apparent, as the pellets were strongly attracted by a permanent magnet (Figure 9, left). Also, both particle loadings could be spun into continuous multifilament yarns without difficulties. No clogging of the spinneret occurred, and

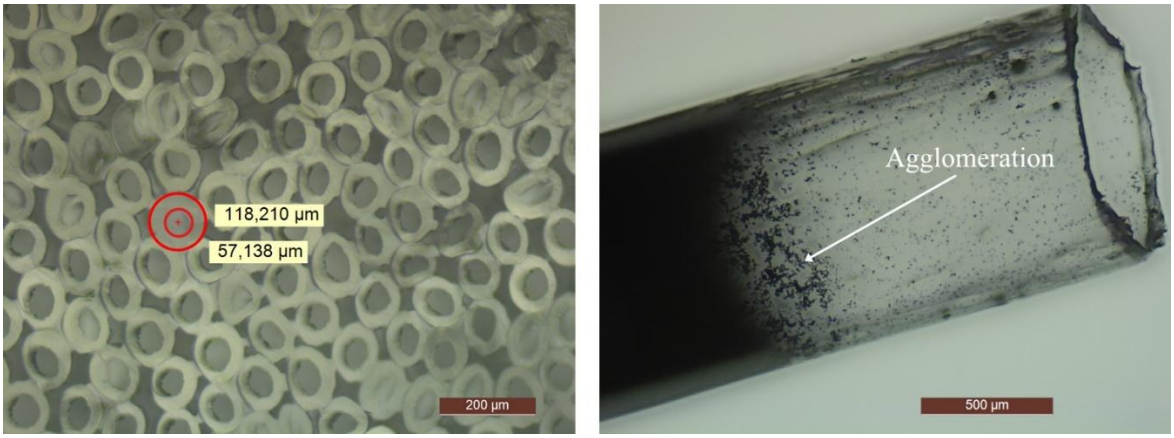

Figure 8. Optical micrographs of liquid-filled hollow fibres. Left: fibres with soybean oil as core material, showing a homogeneous and continuous liquid core. Right: fibre with an iron oxide–oil suspension, revealing inhomogeneous particle distribution and agglomeration within the fibre core.

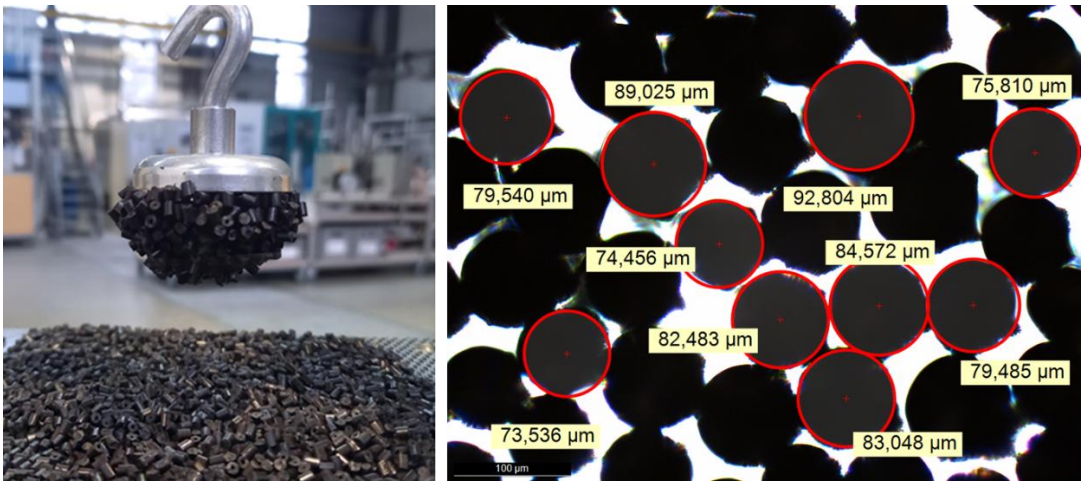

Figure 9. Magnetisable polypropylene compounds and fibres produced from them. Left: polypropylene compound pellets containing Bayoxide E® 8706 nanoparticles (30 wt%) showing strong attraction to a permanent magnet. Right: optical micrograph of cross-sections of fibres spun from the same compound, exhibiting uniform diameters (70–95 µm) and smooth surfaces, indicating homogeneous particle distribution within the polymer matrix.

the filaments exhibited smooth surfaces without visible protruding particles, indicating that the nanoparticles were well embedded in the polymer matrix. In addition, the use of solid-state compounding enabled a higher specific particle loading compared to liquid filling, while maintaining the process stability required for large-scale fibre production.

Optical microscopy of the fibre cross-sections confirmed the uniformity of the produced fibres (Figure 9, right). The fibres exhibited round, homogeneous cross-sections with smooth surfaces and no evidence of particle agglomeration. For fibres with 30 wt% particle content, the measured fibre diameters were in the range of 70–95 µm. These fibres correspond to one of the larger fibre types produced in this study. For subsequent magnetic force measurements, additional fibre types with smaller diameters (30 µm, 45 µm, and 65 µm) were also produced and analysed to assess the effect of fibre thickness on magnetisability.

These results demonstrate that the selected process parameters are suitable for production of magnetisable polypropylene fibres with stable dimensions, well-defined iron content and homogeneous morphology. The resulting fibres were successfully used as reference material in the magnetic detachment force measurements.

Magnetic force measurements

To evaluate the magnetic responsiveness of the fibres, the magnetic attraction force was measured using the custom-built test stand described in the Method section. Six different fibre types were examined, combining three fibre diameters (30 µm, 45 µm, 65 µm) with two particle loadings (20 wt% and 30 wt%). As displayed in Figure 10, the variation of results of repeated measurements on the same test specimen (indicated by the error bars) is in average ±2.89%. This represents the uncertainty of the measurement setup.

The variation among different test specimens is displayed in Figure 11, based on the average of three test per specimen. The box plots represent average value (X), median value (horizontal bar within the box) and first / third quartile (upper and lower box limit).

Again, the variations are small, but as to expect slightly larger than the variations of repeated specimen tests. The number of tests here is too small to allow statistically safe descriptions of the distribution type, but in general it can be stated that the variations are small and in general close to standard distribution. This allows to express the results as average of all nine single values per sample: three specimens, each tested three times.

The measured magnetic forces of all samples are summarised in Figure 12, using the type of evaluation described above. Concerning the mono-component polypropylene fibres, a clear dependence of magnetic force on both particle concentration and fibre diameter is visible. In general, fibres with higher particle loading (30 wt%) generated significantly stronger magnetic forces than those with 20 wt%, confirming that the iron oxide content within the polymer matrix directly affects the magnetic response. The forces measured range from 11.4 ±0.7 mN (30 µm fibre) to 15.6 ±0.7 mN (65 µm fibre) for 20% iron content and from 13.6 ±0.8 mN (30 µm fibre) to 26.6 ±1.8 mN (65 µm fibre) for 30% iron content. For both concentrations, an increase in fibre diameter led to higher measured forces. This effect can be attributed to the higher total magnetic volume per fibre and the resulting increase in magnetic flux density at the fibre surface.

The horizontal green line in Figure 12 represents the magnetic force (17.0 ±0.8 mN) measured for a manually ferrofluid-filled hollow fibre. Compared to the different mono-component fibres serving as reference, this would represent a fibre with 30% iron loading at the diameter of 41 µm. The results demonstrate that magnetisable liquid-filled hollow fibres can achieve equal magnetic forces compared to the solid particle-loaded fibres, while separating the magnetisable particles completely from the environment.

The magnetic force measurements confirmed that the magnetisable polypropylene fibres developed in this study exhibit a clear dependency of magnetic response on both fibre diameter and particle loading. Fibres with higher particle contents (30 wt%) showed distinctly stronger magnetic attraction than those with 20 wt%, which can be attributed to the higher proportion of magnetisable material and the correspondingly stronger interaction with the external magnetic field. In addition, fibres with larger diameters generated higher magnetic forces, indicating that the total magnetic volume per fibre plays a decisive role in the observed behaviour.

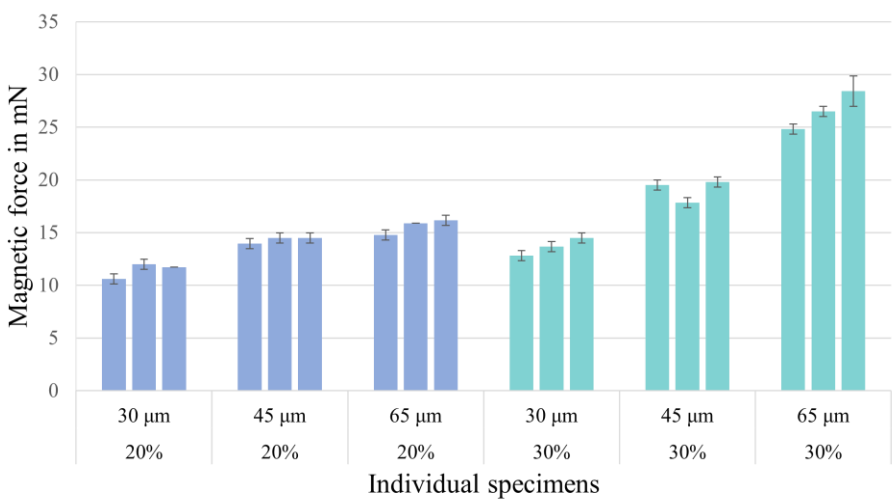

Figure 10. Comparison of the magnetic force of all individual specimens indicating the reproducibility of mesurements.

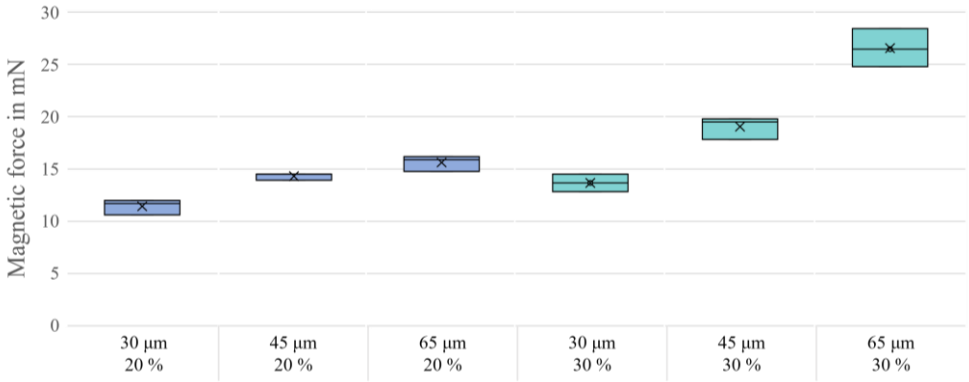

Figure 11. Comparison of the magnetic force of the test specimens per fibre type, indicating the influence of specimen quality.

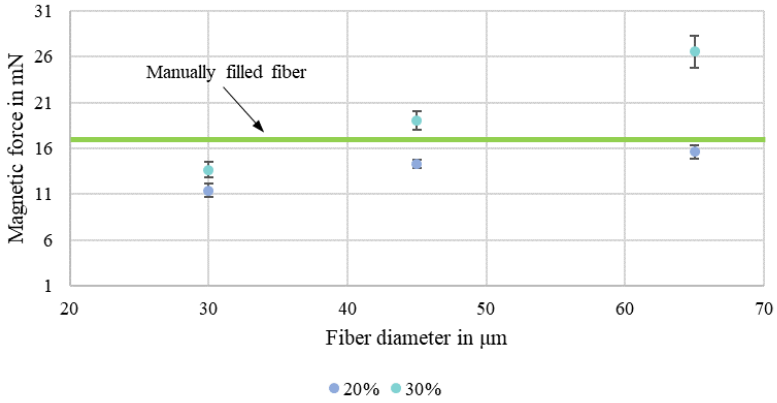

Figure 12. Magnetic force of magnetisable polypropylene fibres as a function of fibre diameter for 20 wt% and 30 wt% particle loading. Error bars represent the standard deviation from three repeated measurements. The green line indicates the magnetic force of a manually ferrofluid-filled hollow fibre used as reference.

A major methodological outcome of this work is the successful development of a dedicated test stand for measuring magnetic attraction forces of individual fibre samples. The system provided reliable, reproducible, and sensitive measurements, enabling a direct comparison of fibres with different compositions and geometries. The obtained data demonstrate that even small differences in fibre structure and particle loading can be quantified with high accuracy.

Overall, the results demonstrate that the magnetisable compound fibres, in combination with the newly developed measurement setup, offer a powerful and reproducible system for studying the magnetic behaviour of polymer-based fibres. Nevertheless, it has to be mentioned, that these results represent a proof-of-concept for the quantification of this type of measurements. For higher statistical safety, influence of the permanent magnet and reproducibility on different set-ups additional research will be necessary.

CONCLUSIONS

In this work, the previously developed melt-spinning process for liquid-filled hollow fibres was adapted and extended to enable the processing of particle-containing core liquids. The process enables the co-extrusion of polymer melts and liquids through a specially adapted spinneret design, allowing the production of fibres with a defined internal liquid core. Using polyethylene and soybean oil as model materials, stable hollow fibres were obtained, proving the general feasibility of the approach.

When magnetisable particles were introduced into the liquid phase, processing challenges such as nozzle clogging and thermal instability of the iron containing fluid occurred. To overcome these limitations, an iron containing fluid with higher thermal stability would be required. Manually filled hollow fibres were instead successfully used as sample material to prove the functionality of magnetisability.

A key outcome of this study is the development of a custom-built measurement unit for quantifying the magnetic attraction force of fibre samples. The test setup proved highly reliable and sensitive, enabling the differentiation of fibre variants based on geometry and magnetic particle content. This novel method allows reproducible magnetic characterisation and establishes a foundation for future systematic studies on polymer-based magnetisable fibres.

Overall, the results demonstrate a new pathway for producing functional hollow and composite fibres with controlled magnetic properties. The combination of innovative fibre manufacturing and the newly developed measurement method represents a step towards the integration of magnetically responsive fibres into technical and smart textile applications.

Acknowledgment: *The authors are much indebted to the federal ministry of economic affairs and climate action for funding this research within the programme INNO-KOM (No. 49VF210033).*

Supported by:

Federal Ministry
for Economic Affairs
and Energy

on the basis of a decision
by the German Bundestag

REFERENCES

1. Kölsch L., Fischer H., Albe C., et al.: Development of Magnetisable Fibres for Reorienting Fibres in Carded Webs by Use of a Magnetic Field. In Team of Authors (eds.): 23rd International Conference STRUTEX (Conference Book). Technical University of Liberec, Liberec, CZ, 2022. ISBN 978-80-7494-621-9, pp. 193 – 196, online: http://strutex.ft.tul.cz/2022/Book/STRUTEX_2022_book.pdf [cit. 03.12.2022].
2. Kölsch L., Fischer H., Kirchhöfer D., et al.: Falona — Faserflornachorientierung. In Series: Forschungsberichte aus dem Faserinstitut Bremen 77. Books on Demand GmbH, Norderstedt, DE, 2024. ISSN 1618-7016. ISBN 978-3-7597-

6176-7. [cit. 13.08.2024].
3. Yang C., Li T., Pei X., et al.: Magnetorheological and Viscoelastic Behaviors in an Fe-Based Amorphous Magnetic Fluid. Materials, 16(5), 2023, article no. 1967. https://doi.org/10.3390/ma16051967
4. Hufenus R., Gottardo L., Leal A.A., et al.: Melt-spun polymer fibers with liquid core exhibit enhanced mechanical damping. Materials & Design, 110(3), 2016, pp. 685 – 692. https://doi.org/10.1016/j.matdes.2016.08.042
5. Kölsch L., Bostan L., Düreth-Joneck S., et al.: Herstellung von gefüllten Hohlfasern als Basis für Filtermodule zur Abwasserreinigung. In Sächsisches Textilforschungsinstitut e.V. (ed.): 16th Symposium „Textile Filter" (proceedings), Chemnitz 2023.
6. Kölsch L., Herrmann A.S.: Bioinspired liquid-filled hollow fibres with shock-absorbing properties. In Zollfrank C., Selhuber-Unkel C. (eds.): 6th Bioinspired Materials 2022 – Proceedings. DGM, St. Augustin, DE, 2022, ISBN 978-3-88355-423-5, 44 P.
7. Pang J.W.C., Bond I.P.: A hollow fibre reinforced polymer composite encompassing self-healing and enhanced damage visibility. Composites Science and Technology, 65(11-12), 2005, pp. 1791–1799. https://doi.org/10.1016/j.compscitech.2005.03.008
8. Röthlisberger M., Dul S., Meier P., et al.: Drug delivery with melt-spun liquid-core fibers. Polymer, 298, 2024, article no. 126885. https://doi.org/10.1016/j.polymer.2024.126885
9. Kling S., Czigány T.: Damage detection and self-repair in hollow glass fiber fabric-reinforced epoxy composites via fiber filling. Composites Science and Technology, 99, 2014, pp. 82–88. https://doi.org/10.1016/j.compscitech.2014.05.020
10. Sigloch H.: Technische Fluidmechanik. 2nd edition, VDI-Verlag Düsseldorf, 1991. ISBN 978-3-18-401017-1.
11. Naeimirad M., Zadhoush A.: Melt-spun Liquid Core Fibers: A CFD Analysis on Bi-phasic Flow in Coaxial Spinneret Die. Fibers and Polymers, 19(4), 2018, pp. 905–913. https://doi.org/10.1007/s12221-018-7902-z
12. Naeimirad M., Zadhoush A., Abrishamkar A., et al.: Melt-spun liquid core fibers: physical and morphological characteristics. Iranian Polymer Journal, 25(5), 2016, pp. 397–403. https://doi.org/10.1007/s13726-016-0431-y
13. Perera A.S., Zhang S., Homer-Vanniasinkam S., et al.: Polymer−Magnetic Composite Fibers for Remote-Controlled Drug Release. ACS Appl. Mater. Interfaces, 10, 2018, pp. 15524−15531. https://pubs.acs.org/doi/abs/10.1021/acsami.8b04774
14. Banerjee H., Leber A., Laperrousaz S., et al.: Soft Multimaterial Magnetic Fibers and Textiles. Adv. Mater., 35, 2023, article no. 2212202. https://doi.org/10.1002/adma.202212202
15. Shahidi S.: Magnetic nanoparticles application in the textile industry—A review. Journal of Industrial Textiles, 50(7), 2021, pp. 970-989. https://doi.org/10.1177/1528083719851852
16. Blachowicz T., Ehrmann A.: Most recent developments in electrospun magnetic nanofibers: A review. Journal of Engineered Fibers and Fabrics, 15, 2020, article no. 1558925019900843. https://doi.org/10.1177/1558925019900843
17. Marx B., Bostan L., Kölsch L., et al.: Development of magnetic sheath-core bicomponent fibers. MRS Communications, 13, 2023, pp. 612–617. https://doi.org/10.1557/s43579-023-00397-4
18. Fu Y., Wei Z., Wan Z., et al.: Recent process of multimode stimuli-responsive flexible composites based on magnetic particles filled polymers: characteristics, mechanism and applications. Composites Part A: Applied Science and Manufacturing, 163, 2022, article no. 107215. https://doi.org/10.1557/s43579-023-00397-4
19. Liao Z., Zoumhani O., Boutry C.M.: Recent Advances in Magnetic Polymer Composites for BioMEMS: A Review. Materials, 16, 2023, article no. 3802. https://doi.org/10.3390/ma16103802
20. Lucarini S., Hossain M., Garcia-Gonzalez D.: Recent advances in hard-magnetic soft composites: Synthesis, characterisation, computational modelling, and applications. Composite Structures, 279, 2022, article no. 114800. https://doi.org/10.1016/j.compstruct.2021.114800
21. Chaudhary B., Winnard T., Oladipo B., et al.: Review of Fiber-Reinforced Composite Structures with Multifunctional Capabilities through Smart Textiles. Textiles, 4, 2024, pp. 391–416. https://doi.org/10.3390/textiles4030023
22. Mamun A., Sabantina L.: Electrospun Magnetic Nanofiber Mats for Magnetic Hyperthermia in Cancer Treatment Applications—Technology, Mechanism, and Materials. Polymers, 15, 2023, article no. 1902. https://doi.org/10.3390/polym15081902
23. Gniotek K., Frydrysiak M., Zieba J., et al.: Innovative textile eletrodes for muscles electrostimulation. In: Proceedings of the 2011 IEEE International Symposium on Medical Measurements and Applications, Bari, Italy, 2011, ISBN 978-1-4244-9336-4, pp. 305–-310. https://doi.org/10.1109/MeMeA.2011.5966678
24. Bica I., Anitas E.M.: Electrical devices based on hybrid membranes with mechanically and magnetically controllable, resistive, capacitive and piezoelectric properties. Smart Mater. Struct., 31, 2022, article no. 045001. https://doi.org/10.1088/1361-665X/ac4ea7
25. Naeimirad M., Zadhoush A., Kotek R., et al.: Recent advances in core/shell bicomponent fibers and nanofibers: A review. J. Appl. Polym. Sci., 135(21), 2018, article no. 46265. https://doi.org/10.1088/1361-665X/ac4ea7
26. Wang S., Xu Q., Sun H.: Functionalization of Fiber Devices: Materials, Preparations and Applications. Adv. Fiber Mater., 4(3), 2022, pp. 324–341. https://doi.org/10.1007/s42765-021-00120-9
27. Bica I.: Composite Materials Based on Polymeric Fibers Doped with Magnetic Nanoparticles: Synthesis, Properties and Applications. Nanomaterials, 12(13), 2022, article no. 2240. https://doi.org/10.3390/nano12132240
28. Safdar F., Ashraf M., Javid A., et al.: Polymeric textile-based electromagnetic interference shielding materials, their synthesis, mechanism and applications – A review. Journal of Industrial Textiles, 51(5_suppl), 2022, pp. 7293S – 7358S. https://doi.org/10.1177/15280837211037085
29. Orasugh J.T., Botlhoko O.J., Temane L.T., et al.: Progress in polymer nonwoven textile materials in electromagnetic interference shielding applications. Functional Composite Materials, 5, 2024, article no. 5. https://doi.org/10.1186/s42252-024-00054-6
30. Fasina O.O., Colley Z.: Viscosity and Specific Heat of Vegetable Oils as a Function of Temperature: 35°C to 180°C. International Journal of Food Properties, 11(4), 2008, pp. 738–746. https://doi.org/10.1080/10942910701586273
31. Roure G.A., Cunha F.R.: Hydrodynamic dispersion and aggregation induced by shear in non-Brownian magnetic suspensions. Physics of Fluids, 30(12), 2018, article no. 122002. https://doi.org/10.1063/1.5058718

DETERMINATION OF FLAX FIBER QUALITY INDICATORS TAKING INTO ACCOUNT SOUND-ABSORBING PROPERTIES FOR ROBOTIC LANDSCAPING SYSTEMS

TOLMACHOV, VOLODYMYR[1]; RIABKO, ANDRII[2*]; HRUDYNIN, BORYS[3]; MARYNCHENKO, YEVHENII[4]; ROZHKOVA, ANASTASIA[5] AND IHNATIEVA, VIKTORIIA[6]

[1] Department of Professional Education and Computer Technologies, Olexander Dovzhenko Hlukhiv National Pedagogical University, Kyivska str. 24, Hlukhiv, Ukraine
[2] Department of Physics and Mathematics Education and Informatics, Olexander Dovzhenko Hlukhiv National Pedagogical University, Kyivska str. 24, Hlukhiv, Ukraine
[3] Physics Department Education and Research Institute of Energetics, Automation and Energy Efficiency, National University of Life and Environmental Sciences of Ukraine, Heroiv Oborony str. 15, Kyiv, Ukraine
[4] Department of Professional Education and Agricultural Production Technologies, Olexander Dovzhenko Hlukhiv National Pedagogical University, Kyivska str. 24, Hlukhiv, Ukraine
[5] Department of Professional Education, Restaurant and Tourist Business, Taras Shevchenko Luhansk National University, Ivan Banka str. 3, Poltava, Ukraine
[6] Department of structural mechanics, Ternopil Ivan Puluj National Technical University, Ruska str. 56, Ternopil, Ukraine

ABSTRACT

The confluence of increasing global sustainability demands and the imperative for real-time quality control in advanced manufacturing systems provides the foundation for this study. We address this by initially conceptualizing an active robotic noise-mitigation panel based on flax fiber designed for autonomous deployment in landscaping and urban noise control environments. The feasibility of this active system, which relies on the dynamic manipulation of a passive flax core integrated with AI-driven sensing and actuation, is fundamentally dependent on precise and rapid assessment of the raw fiber's acoustic potential and physico-mechanical quality. Confronting the scarcity of suitable non-destructive pre-assessment techniques, this paper details the subsequent development and comprehensive validation of a novel methodology utilizing the sound absorption effect to characterize flax fiber quality. A specialized device was engineered and rigorously optimized, establishing critical operational parameters: a 10 g sample mass, an emitter frequency of 1750 Hz (optimally aligned with the λ/4 thickness), and a reference moisture content of 12%. The research successfully established a robust statistical correlation between the acoustic attenuation measurements and key industrial indicators, specifically linear density, breaking load, and flexibility. Statistical validation using the Student's t-test confirmed a high degree of agreement with established standards (DSTU 4015-2001), demonstrating excellent reproducibility and high precision (relative expanded uncertainty below 5 %). Furthermore, empirical power and logarithmic regression formulas were derived to enable the direct calculation of quality parameters from the acoustic data. This integrated approach not only provides a reliable, rapid, and objective tool for industrial quality control, but also furnishes the essential material assessment capability required to transition sustainable flax materials into the demanding domain of smart, active noise-mitigation technologies.

KEYWORDS

Active noise mitigation; Breaking load; Flax fiber; Linear density; Non-destructive testing; Quality control; Sound absorption; Sustainable materials.

INTRODUCTION

Flax fibers play a significant role in modern technology and production due to their exceptional mechanical properties, biodegradability, and sustainability. They are widely used in the textile industry, composite materials, automotive manufacturing, and eco-friendly packaging. The growing demand for natural and renewable materials highlights the need for simple and effective methods to assess the physical and mechanical properties of flax fibers.

Robotic landscaping systems represent an emerging technological direction within smart urban infrastructure and automated environmental management. Such systems may include autonomous service robots, adaptive architectural elements, and intelligent environmental control units

* **Corresponding author:** Riabko A.V., e-mail: *ryabko@meta.ua*
Received October 30, 2025; accepted April 10, 2026

designed to improve comfort in public and residential spaces. In the context of noise management, robotic systems can deploy mobile or reconfigurable acoustic panels that dynamically adapt their position, orientation, or configuration in response to changing acoustic conditions. Natural fibrous materials, particularly flax fiber, are promising candidates for such applications due to their low density, porosity, and high sound absorption capability. The effectiveness of these acoustic elements largely depends on the structural parameters of the fibrous layer, including fiber fineness, packing density, flexibility, and internal pore structure, which determine the mechanisms of acoustic energy dissipation within the material.

However, the successful integration of flax-based acoustic materials into such robotic noise-control systems requires reliable and rapid methods for evaluating the quality of the raw fibrous material. The acoustic performance of fibrous layers is strongly influenced by the physico-mechanical properties of the fibers, including linear density, flexibility, and structural uniformity. Therefore, the development of simple, efficient, and non-destructive methods for assessing these parameters is an important task both for industrial quality control and for the design of advanced acoustic systems based on natural fibers.

Flax fiber-based panels are increasingly considered for use in robotic noise control systems due to their natural sound-absorbing properties. Such systems include mobile or adjustable panels in urban environments, smart buildings, and public spaces that autonomously reduce noise by optimizing panel placement and orientation. Given the wide range of potential applications, from city landscaping to interior acoustic management, it becomes crucial to develop simple and effective methods for assessing the physical and mechanical properties of flax fibers, particularly their sound absorption capabilities. Efficient evaluation techniques would ensure consistent quality and performance of flax-based acoustic materials in these advanced robotic systems. Reliable and rapid evaluation techniques can improve quality control, optimize production processes, and enhance the performance of flax-based materials in various applications. The development of non-destructive testing methods, such as those based on sound absorption, provides an innovative and efficient approach to fiber characterization, supporting advancements in both scientific research and industrial applications.

The analysis of indirect methods for determining the linear density of fiber based on air flow passage and illumination of a prepared fiber sample with a light beam indicates that some similarities can be found in the fundamental principles of these methods. According to the method of determining linear density by air flow passage, fiber samples of the same mass are used for research, the air pressure is also kept constant, and only the piston descent speed or the float rise height is recorded, both of which depend on the fiber thickness. Thus, the thinner the fiber, the slower the air passes through it. A similar phenomenon is observed when light and sound pass through the material - the thinner the fiber, the more it obstructs sound transmission or scatters and absorbs light. In this way, the absorption coefficient of the investigated material is determined [1].

The effect of energy loss by a sound wave as it passes through a material is used in many measuring instruments and various fields to determine the physico-mechanical properties of the studied materials, such as evaluating sound insulation efficiency or assessing the properties of fibrous and composite materials.

In the case of fibrous materials, it is necessary to consider that the acoustic properties of such a material depend on the properties of the fibers, the properties of the surrounding space, and the properties of the contacts between the fibers.

For a rapid assessment of fiber quality, the method of determining its sound absorption capacity can be used. In our study, we propose a method based on measuring the intensity of sound vibrations of a specific frequency that pass through a fiber sample of a defined mass. This study explores an alternative approach by utilizing the sound absorption effect to assess fiber quality, offering a rapid and non-destructive method. The originality of this approach lies in its ability to indirectly determine fiber density and structural uniformity through acoustic wave interaction, providing a novel perspective on fiber characterization.

LITERATURE REVIEW

In recent years, natural fibers, particularly flax fibers, have attracted growing interest among researchers due to their unique sound-absorbing properties. These characteristics make them suitable for the development of acoustic panels aimed at reducing noise in urban environments, residential buildings, and robotic landscaping systems. Beyond their technical advantages, such materials also offer environmentally friendly alternatives to synthetic absorbers, combining sustainability with practical applications for improving the quality of human living spaces.

An equally important research direction is the search for effective and straightforward methods to determine the physico-mechanical properties of flax fiber based on its sound-absorbing behavior. Such approaches not only simplify quality assessment but also provide rapid and non-destructive alternatives to traditional techniques. This makes them highly relevant for modern applications, where efficiency, precision, and sustainability are increasingly valued. In recent years, numerous scientific studies have focused on the utilization of flax fibers and the

development of methods for analyzing their properties. Zhixiong Bi et al. studied the effect of voids on the sound absorption of 3D printed flax fiber reinforced PLA composites (CFFRCs). Using impedance tube measurements and numerical simulations, they found that voids inside flax yarns enhance absorption by increasing viscous friction, while voids between yarns reduce performance by altering sound propagation. The results provide insights for optimizing the acoustic properties of 3D printed flax fiber composites [2].

Sathesh Babu M et al. investigated the impact of Mahua oil cake microcellulose (MOCM) on the mechanical and sound absorption properties of flax fiber-reinforced polymer composites. The study found that adding 7.5 wt.% MOCM optimally enhanced tensile, flexural, and impact strength, while increasing MOCM content improved sound absorption. The findings highlight MOCM as a sustainable filler for enhancing both structural and acoustic performance in composite materials [3].

Diwahar Periyasamy et al. investigated the recycling potential of waste HDPE films reinforced with flax fiber to create sustainable decorative tiles. The study analyzed mechanical, thermal, water absorption, and sound absorption properties, revealing that adding natural fibers improved tensile and flexural strength by up to 25% and impact strength by 38%. SEM analysis confirmed enhanced interfacial bonding, supporting the conclusion that HDPE/natural fiber composites offer a sustainable alternative for decorative tile production [4].

V. Bhuvaneswari et al. conducted a critical review of the hygrothermal and sound absorption behavior of natural-fiber-reinforced polymer composites, emphasizing their eco-friendly benefits and challenges. The study examined moisture absorption characteristics, highlighting the need to convert hydrophilic fibers into hydrophobic ones to enhance mechanical and thermal properties. Additionally, the review found that composites with greater thickness, porosity, and density exhibited superior sound absorption performance [5].

Andi Harisa et al. investigated the effects of moisture absorption on the mechanical and acoustic properties of flax/polypropylene (PP) composites. The study found that water uptake followed Fickian behavior in flax/PP at room temperature, while flax-carbon/PP hybrids exhibited deviations, with carbon fiber hybridization reducing water absorption by 25%. Moisture exposure significantly decreased stiffness and resonant frequency, while tensile strength remained largely unaffected, impacting the composite's acoustic performance [6].

Eulalia Gliscinska et al. investigated the sound absorption properties of biodegradable thermoplastic composites made from flax and polylactide fibers. They analyzed the effects of multilayer structures, profiling, and the arrangement of composite layers on sound absorption performance using a Kundt tube. The study found that profiling the composite plate and adding pre-pressed nonwoven layers improved sound absorption, shifting the peak absorption range toward lower frequencies [7].

Mohammadi M. et al. reviewed recent advancements in the use of natural fiber-reinforced composites as sound-absorbing materials, highlighting their acoustic, mechanical, and thermal properties. They examined different composite structures, chemical treatments, and nanomaterial coatings to enhance sound absorption efficiency. The study emphasized the environmental benefits of replacing synthetic materials with sustainable, cost-effective, and recyclable natural fibers, addressing noise pollution and ecological concerns [8].

Abhijit Kudva, Mahesha Gt, Dayananda Pai, Ian Philip Jones of reviewed the physical, thermal, mechanical, sound absorption, and vibration damping properties of natural fiber-reinforced and hybrid fiber-reinforced polymer composites. Their study highlighted that natural fiber composites exhibit enhanced sound absorption and vibration damping characteristics, making them suitable for acoustic applications. Additionally, combining natural and synthetic fibers was found to improve the overall mechanical performance of the composites [9].

Madushika and Lanarolle reviewed novel approaches to improving the sound absorption performance of textile fibers as alternatives to conventional soundproofing materials. They examined chemical modifications, such as plasma and alkali treatments, and physical modifications, including microfibers, nanofibers, hollow fibers, and aerogel-treated fibers. Their findings indicate that these modifications enhance sound absorption by increasing fiber surface area, roughness, and material tortuosity, with treated natural fibers achieving absorption coefficients up to 0.9 at mid and high frequencies [10].

Gumanová et al. investigated the sound absorption properties of natural fibers—cork, hemp, and fiberboard—compared to conventional insulating materials like mineral wool, propylat, and polyurethane foam. Using the impedance tube method (ISO 10534-2), they measured the sound absorption coefficient across different material thicknesses and frequencies. Their findings showed that hemp exhibited the highest absorption ($\alpha = 0.99$ at 2000 Hz, 20 mm thickness), while cork had the lowest performance at low frequencies, with mineral wool performing best among conventional materials [11].

Su et al. investigated the mechanical, thermal, and sound isolation properties of a novel three-dimensional orthogonal woven sisal/flax hybrid fiber biocomposite (3DOWSBCs). They compared its performance to traditional laminated composites and used a finite element model (FEM) to analyze the strengthening effects of Z-yarns. Their results

showed that 3DOWSBCs exhibited significantly improved flexural and shear strength, along with low thermal conductivity (0.29 W/m·K) and high sound transmission loss (63 dB), highlighting their potential for sustainable industrial applications [12].

Rotini et al. investigated the acoustic properties of polylactic acid (PLA) foam composites reinforced with plant fibers, specifically grape stems and wood straw, for sound insulation applications. They conducted acoustic tests to evaluate absorption, reflection, and impedance, analyzing different material configurations and thicknesses. Their findings highlight the potential of these eco-friendly composites for sustainable construction, emphasizing the influence of plant fiber characteristics on acoustic performance [13].

Liang et al. reviewed the sound absorption mechanisms, material modifications, and structural designs of synthetic fiber materials for industrial noise reduction, addressing their limitations in absorption coefficient and frequency range. They analyzed predictive models like Delany-Bazley and Johnson-Champoux-Allard (JCA), highlighting differences in how they account for air viscosity and thermal conduction. The study also explored methods to enhance the acoustic properties of polymers, metal fibers, and inorganic fibers through structural modifications, material combinations, and advanced fabrication techniques [14].

Eun-Suk Jang summarized studies on sound-absorbing green materials from agricultural by-products, such as flax and nettle fibers. The review highlighted thickness, density, and air cavity as key factors determining acoustic performance [15].

Daira Sleinus et al. developed eco-friendly composites from flax fiber, sphagnum moss, vermiculite, and sapropel for sound absorption and moisture buffering. The study showed that flax fiber–vermiculite composites provided more stable sound-absorbing and mechanical properties than other mixtures, confirming the potential of flax fiber as a sustainable acoustic material [16].

Tao Yang et al. reviewed the sound absorption properties of natural fibers as sustainable alternatives to synthetic materials. They emphasized that many natural fibers, including flax, can achieve sound absorption comparable to glass fiber while being safer for human health and more environmentally friendly. The review highlights flax fiber as a promising candidate for eco-friendly acoustic applications, particularly in sustainable construction and noise control systems [17].

This review highlights the growing interest in utilizing flax fibers for sound absorption applications, particularly within sustainable composite materials designed for urban and architectural noise mitigation, including advanced robotic systems. Various studies have investigated factors such as fiber structure, moisture absorption, and the inclusion of fillers to enhance sound absorption performance. Innovative approaches like 3D printing, hybrid fiber combinations, and the use of biodegradable matrices, such as PLA, have been extensively explored to enhance the acoustic and mechanical properties of flax-based composites, providing potential solutions for sustainable construction and industrial noise reduction. However, while the acoustic performance of the final flax-based product is well-documented, the literature reveals a significant gap regarding rapid, non-destructive, and straightforward methods for determining the initial physico-mechanical quality indicators of the raw flax fiber itself, which fundamentally dictates the final product's sound-absorbing potential.

RESEARCH METHODOLOGY

Our work is centered on the development of an active robotic noise-mitigation panel based on flax fiber designed specifically for landscaping and urban noise control systems. The fundamental concept integrates the sustainable, natural acoustic properties of flax with real-time, adaptive robotic control to achieve superior noise reduction efficiency. The panel's architecture is anchored by the flax fiber sound-absorbing layer, which forms the core of its passive noise reduction capability. This layer may be deployed as pure flax or integrated into a biopolymer composite to enhance structural integrity and longevity. A noise sensor module, comprising micro-microphones and acoustic transducers, continuously surveys the ambient environment, providing real-time data on the noise intensity and its frequency spectrum. This input is fed directly to the Controller/Artificial Intelligence Module, which instantly analyzes the current configuration's efficacy and calculates the optimal adjustments required to maximize absorption (Figure 1).

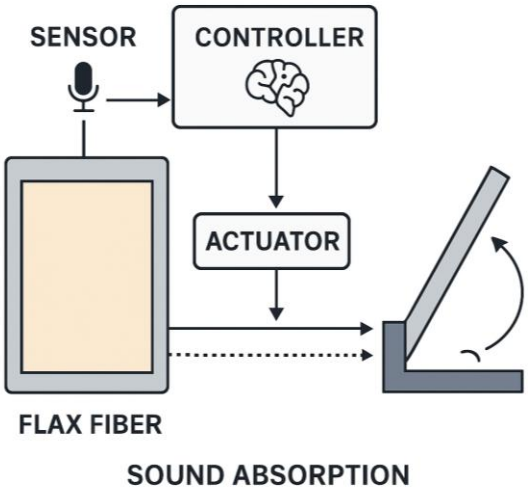

Figure 1. Conceptual diagram illustrating the operating principle of the active robotic noise-mitigation panel based on flax fiber.

Physical adaptation is achieved by actuating elements, such as servomotors or piezoelectric components. These effectors dynamically manipulate the panel's position, altering its tilt, distance from the noise source, or, where necessary, adjusting the configuration of auxiliary acoustic chambers designed to selectively enhance the absorption of lower frequencies through resonance. The entire functional apparatus is supported by a robust panel frame and structural support, guaranteeing mechanical stability and facilitating the necessary range of motion and configurational changes. The operating cycle is continuous: noise is detected, analyzed, and the panel is actively adjusted to maintain optimal absorption, creating a perpetual feedback loop that adapts to shifting noise profiles.

It is during this foundational development phase, particularly in designing the flax-based core and validating its acoustic performance for robotic deployment, that we encountered a critical necessity: the existing methods for rapid quality assessment were insufficient. This challenge compelled us to develop and validate a dedicated, non-destructive technique for determining the sound-absorbing properties of the flax fiber itself, an innovative methodology that is detailed in the subsequent sections of this article.

For rapid assessment of flax fiber quality, the method of determining its sound absorption capacity can be used. Based on the obtained results, the fiber can be objectively characterized by properties such as flexibility, linear density, and tensile strength. The proposed method is based on measuring the intensity of sound vibrations of a specific frequency passing through a fiber sample of a defined mass. The measurement is conducted in a sealed cylindrical chamber of constant volume, which eliminates the influence of external environmental sounds on the measurement results.

Based on the research findings, a device was designed to determine the degree of sound wave absorption by fibrous material. Its operating principle is based on determining the sound pressure level as the sound wave passes through a specific volume of fibrous material. The intensity of the sound wave passing through the material is monitored by an acoustic sensor—a condenser microphone. The measured sound signal is then linearly converted into a direct current, the voltage of which is processed by a microcontroller, and the result is displayed on a digital screen. Figure 2 shows the structural diagram of the developed device.

Figure 3 shows the functional diagram of the device. The device consists of the following main elements: a controlled sinusoidal oscillator, a low-frequency amplifier, an emitter, a measurement chamber with the tested material, a sound signal sensor, an amplifier, an amplitude detector, and a specialized signal processing circuit.

The determination of sound pressure is carried out by an acoustic sensor (e.g., a condenser microphone), which is connected to a specialized sound processing circuit. This circuit is responsible for signal amplification and subsequent linear conversion of the alternating acoustic signal into a constant voltage, which is then fed into an Analog-to-Digital Converter (ADC). In our implementation, the data is typically fed into an analog input pin of the Arduino Nano microcontroller. The obtained digital data is processed by the microcontroller according to the developed algorithm, and the final calculation results are displayed on a digital screen. The signal amplifier within the device is calibrated so that the maximum measurable sound pressure value corresponds to 5 V (the maximum analog reference voltage of the Arduino Nano), which the 10-bit ADC then digitizes into 4095 relative units (ranging from 0 to 1023, assuming a standard 10-bit ADC resolution for 5 V). Figure 4 presents the circuit diagram of the device.

The acoustic properties of flax raw material were analyzed using the developed device (Figure 5). The device consists of a plastic housing (1), a sound emitter (4), an acoustic sensor (6), and a measurement chamber (5). Inside the housing are the electronic sound processing module and the sound frequency generator (2), an amplifier, a digital indicator (3), and control buttons. For the study, a 10 g fiber sample is cut into approximately 2 cm pieces, placed into the measurement chamber (5), and then inserted into the device (Figure 6).

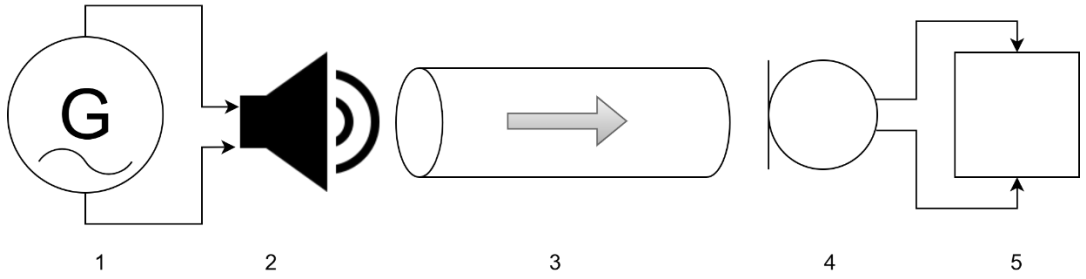

Figure 2. Structural diagram of the device for determining the sound absorption coefficient: 1 – generator; 2 – sound emitter; 3 – measurement chamber with the tested material; 4 – sound sensor; 5 – signal processing and result display unit.

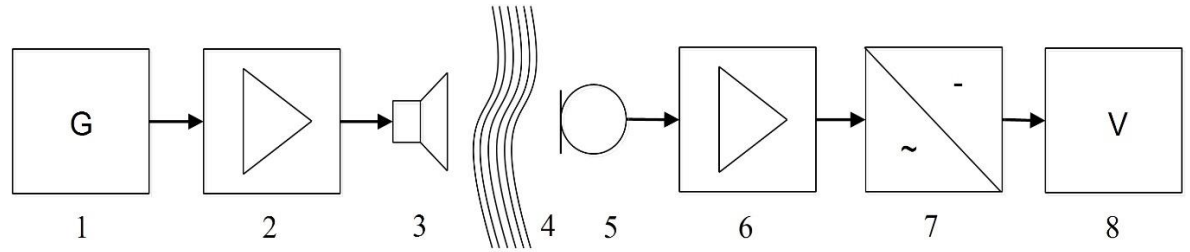

Figure 3. Functional diagram of the device for determining the sound absorption coefficient: 1 – generator; 2 – signal amplifier; 3 – sound emitter; 4 – tested material; 5 – sound sensor; 6 – signal amplifier; 7 – amplitude detector; 8 – signal processing and measurement display unit.

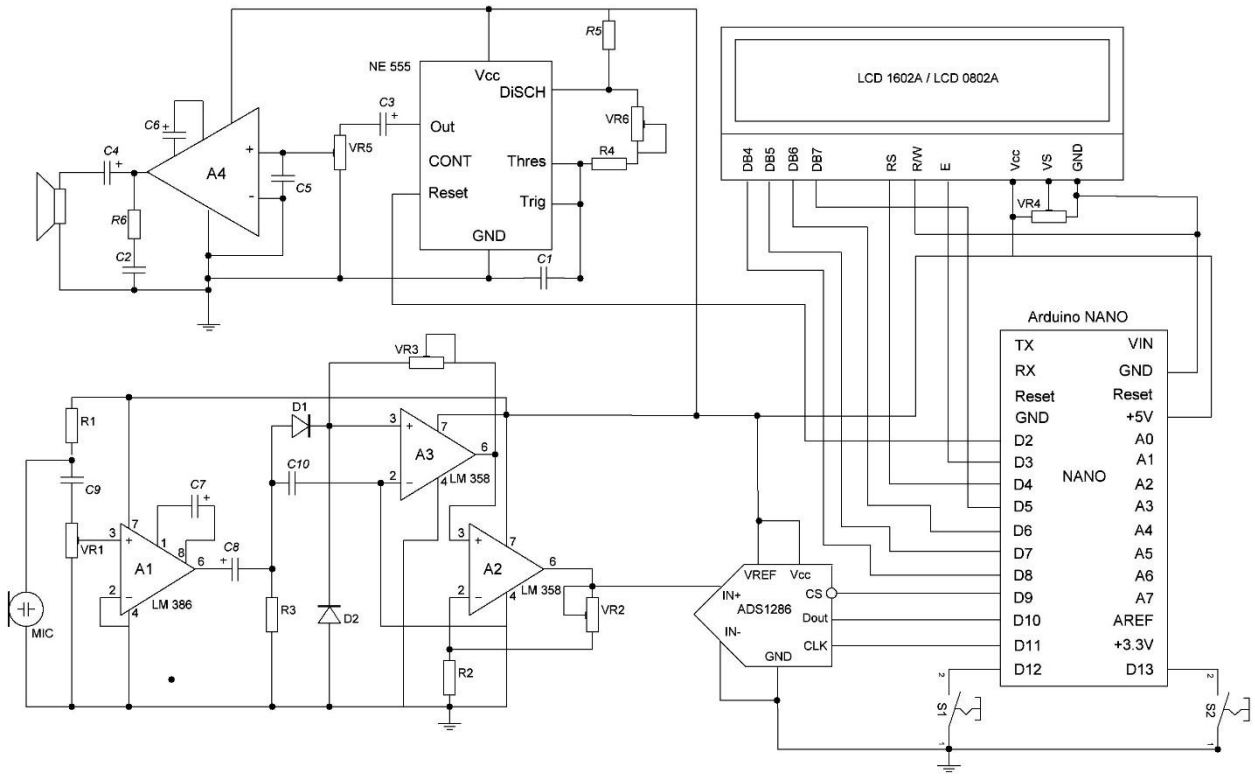

Figure 4. The circuit diagram of the device.

Using the control buttons, the desired operating mode is selected according to the developed algorithm, and the measurement is performed. The measurement result is taken as the arithmetic mean of ten samples from the same batch, calculated to the second decimal place and then rounded to the first decimal place. The device is powered by a 12 V DC source with a current of at least 0.25 A.

The developed device algorithm has a combined structure, integrating a control button processing unit and an operation mode selection unit. It includes several modes: 1) Emitter Testing Mode – Verifies the generator, amplifier, emitter, acoustic sensor, and digital circuit. It allows sound absorption analysis within a selected frequency range or a default range (500 Hz–2000 Hz, step 50 Hz); 2) Frequency Range Selection Mode – Sets the working frequency range for material analysis; 3) Measurement Mode – Conducts multiple measurements with statistical processing; 4) Result Display Mode – Shows measurement results on the digital display.

To evaluate quality using the developed device, it is necessary to determine its parameters and those of the fiber sample. Key parameters include the emitter's operating frequency and the sample mass. The device's algorithm provides test and working modes to select and apply a specific emitter frequency or a frequency range for further analysis.

The cross-sectional size of the measurement chamber depends on the device's design, with the fiber length for analysis being approximately 80% of the chamber diameter (28–30 mm). To determine the sample mass and emitter frequency, an analysis of the empty measurement chamber was conducted

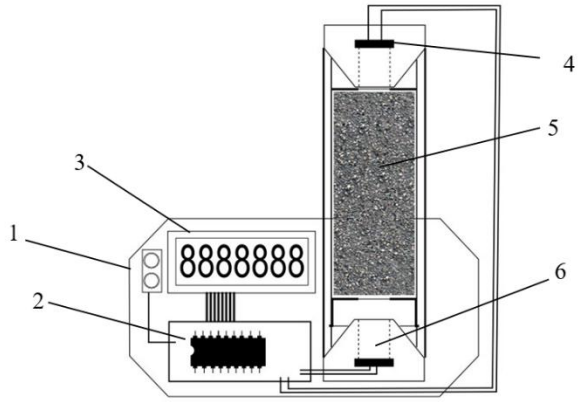

Figure 5. Schematic diagram of the device: 1 – housing; 2 – sound signal processing module and frequency generator; 3 – digital display; 4 – sound emitter; 5 – measuring chamber with fiber; 6 – acoustic sensor.

Figure 6. Device appearance: 1) in operating condition; 2) with the measuring chamber removed.

across the working frequency range (500–2000 Hz) with a step of 50 Hz. The results indicate that as the emitter frequency increases, the sound pressure on the acoustic sensor (a microphone) decreases.

Each measurement was repeated ten times. The presented values correspond to the mean value of the measurements. The number of repetitions was determined based on preliminary statistical analysis, ensuring that the relative experimental error did not exceed 5%.

Prior to measurement, flax fiber samples were conditioned to a standard moisture content of 12%, according to the requirements of the relevant standards for flax fiber testing. For each measurement, a sample with a mass of 10 g was prepared. The fibers were cut to a length of approximately 28–30 mm, which corresponds to about 80% of the diameter of the measuring chamber. The length of the prepared flax fibers was approximately 80% of the diameter of the measuring chamber, which ensured uniform filling of the chamber volume and provided controlled geometric conditions for the acoustic measurements.

The prepared fiber sample was loosely placed into the cylindrical measuring chamber of constant volume without forced alignment of individual fibers. This approach results in a randomly oriented but reproducible fibrous structure that reflects the natural arrangement of fibers in bulk material. To minimize the influence of spatial orientation on the acoustic response, the measurements were performed with ten repetitions and the results were statistically averaged.

Such a preparation procedure ensures comparable packing density and consistent experimental conditions for all tested samples. To minimize the possible influence of spatial fiber orientation on the acoustic response, each measurement was repeated ten times, and the final values were calculated as the average of the obtained results.

To determine the optimal sample mass for analysis, two fiber batches with the lowest and highest linear densities were selected. Measurements were conducted using samples of 5, 10, and 15 g, with each measurement repeated ten times.

The results indicate that 5 g samples have minimal impact on the intensity of the sound wave reaching the acoustic sensor (Figure 7, Figure 8). However, as the sample mass increases, the density of the measurement chamber filling rises, enhancing sound absorption, which is evident at 10 g and 15 g. Due to the chamber's design, samples exceeding 15 g cannot be accommodated.

For 15 g samples, the absorption curve for low-density fibers rapidly approaches zero at emitter frequencies above 1550 Hz, leading to inaccurate measurements. In contrast, 10 g samples provide nonzero readings up to 1900 Hz, making this mass the optimal choice for further measurements (Figure 7).

To determine the required operating frequency range of the emitter, two batches of fiber with the lowest and highest linear density values are selected, and measurements are performed on pre-prepared samples weighing 10 g. The graphical representation of the experimental results is shown in the Figure 9.

Analyzing the obtained data, it can be determined that noticeable attenuation of the sound wave when using samples with different linear densities begins at an emitter frequency of 1400 Hz, although at this frequency the difference between the device readings is minimal. In the emitter frequency range of 1650–1850 Hz, the maximum difference in device readings is observed when testing samples with the most contrasting linear densities.

The selection of the operating frequency and the sample mass was based on preliminary experimental studies carried out using the developed device. Measurements were performed within a frequency range of 500–2000 Hz with a step of 50 Hz in order to determine the most informative working frequency. The analysis showed that the difference between the readings obtained for flax fibers with significantly different linear density becomes most pronounced in the frequency range of 1650–1850 Hz. Therefore, the working frequency of 1750 Hz, corresponding to the middle of this range, was selected for further measurements.

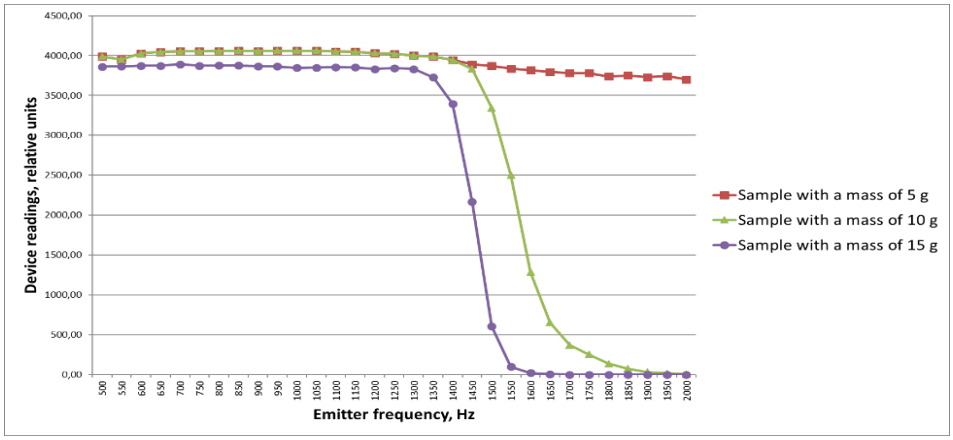

Figure 7. Dependence of the device readings on the emitter frequency for samples of different masses with the lowest linear density.

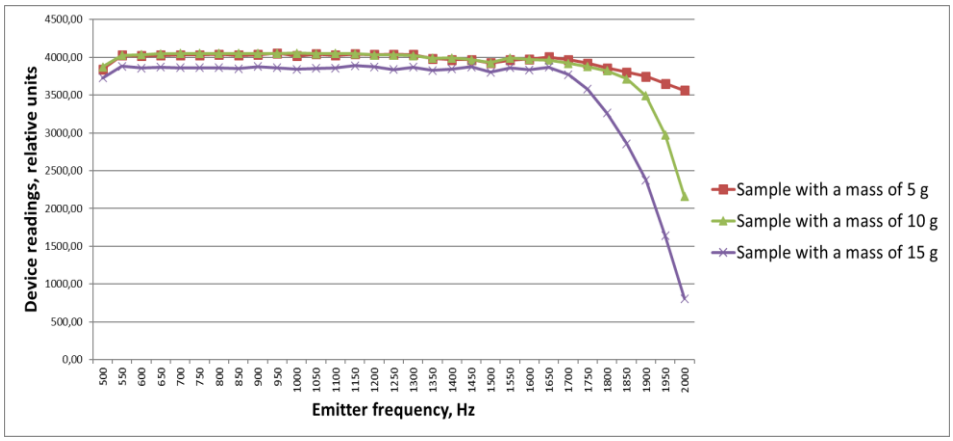

Figure 8. Dependence of the device readings on the emitter frequency for samples of different masses with the highest linear density.

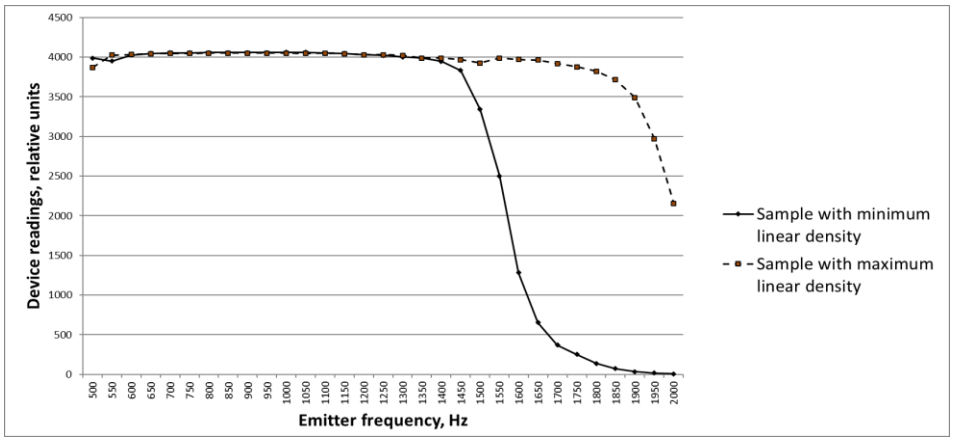

Figure 9. Dependence of device readings on emitter frequency for samples with different linear densities.

The mass of the tested samples was determined experimentally by comparing measurements performed with samples of 5 g, 10 g, and 15 g. It was observed that samples with a mass of 5 g had only a minor effect on the acoustic signal passing through the measuring chamber. At the same time, samples with a mass of 15 g led to excessively strong attenuation of the acoustic signal at higher frequencies, resulting in near-zero readings and reduced measurement sensitivity. A sample mass of 10 g provided stable and informative readings across the investigated frequency range and was therefore selected as the optimal value for further experiments.

The obtained results demonstrate that at the selected operating frequency of 1750 Hz the device readings show the highest sensitivity to variations in fiber linear density, which allows reliable differentiation of flax fiber samples with different fineness.

Sound absorption in porous materials occurs due to viscous forces that impede air movement through pores, causing part of the kinetic energy of oscillating air particles to dissipate as heat. The absorption efficiency depends on air viscosity and density, pore geometry, and material thickness.

The effect becomes significant at frequencies where oscillating air particles transfer energy to the porous

structure. For effective absorption, the sample thickness should equal at least one-quarter of the wavelength. In this study, the optimal emitter frequency was selected as 1750 Hz, corresponding to a wavelength of 0.19 m, which defines an effective sample thickness or chamber length of about 48 mm.

In order to obtain reliable experimental data using the developed device, based on determining the intensity of the sound wave after passing through the tested fiber sample, it is necessary to establish the required number of repeated measurements.

For this purpose, samples from five batches of flax fiber with different values of linear density were prepared and measured using the developed device with repeated measurements. The obtained experimental data were mathematically processed. Based on a predetermined relative experimental error of 5%, the minimum number of repetitions required for each sample was calculated.

The results of this analysis are presented in Table 1.

Analysis of the data presented in Table X shows that, in order to obtain reliable measurement results and to ensure objective evaluation of the physico-mechanical characteristics of flax fibers, the experiments should be performed with ten repetitions. Under these conditions, the relative experimental error does not exceed 5%. Therefore, all experimental results presented in this study represent the mean values obtained from ten repeated measurements.

To ensure reliable results, fiber samples from five batches with different linear densities were tested on the device, and the data were statistically processed. At a relative error of 5%, the required number of repetitions for each sample was determined. The analysis showed that to obtain objective measurement results and evaluate the physico-mechanical properties of the tested material, experiments should be performed with ten repetitions, ensuring that the relative error does not exceed 5%.

To determine the effect of the actual moisture content of the tested fiber on the instrument readings, measurements were carried out using fiber samples with varying moisture levels. The measurements were performed with different repetitions according to the above recommendations. Since the actual moisture content of scutched flax used in production is 12%, and considering that all previous experiments were conducted at this level, 12% was taken as the reference value. Measurements were then performed with samples having moisture contents ranging from 8% to 20%, adjusted in 4% increments through artificial humidification and drying.

The analysis of measurement results showed that as the actual fiber moisture increased from 8% to 20%, the instrument readings rose from 1285 to 3718 relative units. This effect can be explained by the reduction in energy losses of the sound wave passing through the tested fiber sample with higher moisture content. Therefore, the optimal moisture content of the fiber suitable for measurements with the developed device should be 12%.

To evaluate the repeatability, accuracy, and uncertainty of the measurements obtained using the developed device, an experimental study was carried out using 30 flax fiber samples with different physical and mechanical properties. Each sample was measured with ten repetitions under identical experimental conditions according to the previously described measurement procedure. The obtained experimental data were statistically processed, and the mean values, standard deviation (σ), standard error of the mean (±m), and coefficient of variation (C, %) were calculated. The results of the statistical processing of the measurements are presented in Table 2.

Analysis of the obtained results shows that the coefficient of variation for most samples does not exceed 8%, which indicates good repeatability of the measurements obtained using the developed device.

To verify the reliability and practical applicability of the developed measurement method, a correlation analysis was performed between the device readings and the main physical and mechanical quality indicators of flax fiber: linear density, flexibility, breaking load, and color group. The correlation coefficients obtained are presented in Table 3.

The obtained results demonstrate a strong correlation between the device readings and the linear density of flax fiber (R = 0.95). Moderate correlations were observed with flexibility and breaking load (R = ±0.68). No statistically significant correlation was found with the fiber color group (R = –0.20).

The results of the statistical and correlation analysis confirm the presence of a significant relationship between the acoustic characteristics measured by the developed device and the main physical-mechanical properties of flax fiber at a significance level of 0.05.

Table 1. Determination of the minimum number of experimental repetitions.

Experimental results	Fiber sample number				
	1	2	3	4	5
Mean device reading, rel. units	3876.7	3841.2	3274.5	348.3	253.3
Standard deviation	46.80	84.05	125.75	21.63	15.31
Coefficient of variation, %	1.27	2.45	4.05	6.55	6.37
Student's t-coefficient			2.26		
Acceptable relative error, %			5		
Required number of experiments	1	2	4	10	9
Total number of experiments			10		

Table 2. Statistical processing of measurement results obtained using the device.

Batch No.	Mean device reading (rel. units)	σ (standard deviation)	±m (standard error)	C [%] coefficient of variation
1	1324.6	51.18	31.72	4.07
2	550.8	42.82	26.54	8.20
3	1250.2	47.74	29.59	4.03
4	1203.4	70.26	43.55	6.15
5	1148.5	90.11	55.85	8.27
6	957.4	75.52	46.81	8.31
7	747.5	49.43	30.64	6.97
8	1121.3	76.19	47.22	7.16
9	1577.4	53.67	33.27	3.59
10	773.7	49.65	30.77	6.76
11	1982.6	82.37	51.05	4.38
12	204.4	14.93	9.26	7.70
13	435.3	25.46	15.78	6.17
14	902.4	52.87	32.77	6.18
15	754.8	39.45	24.45	5.51
16	1343.0	70.43	43.65	5.53
17	985.3	69.02	42.78	7.38
18	3876.6	66.43	41.17	1.81
19	1533.0	65.39	40.53	4.50
20	677.7	44.05	27.30	6.85
21	422.7	32.59	20.20	8.13
22	253.3	15.31	9.49	6.37
23	554.8	42.52	26.36	8.08
24	450.9	35.07	21.74	8.20
25	181.5	14.45	8.96	8.39
26	391.9	19.55	12.12	5.26
27	552.4	38.29	23.73	7.31
28	652.5	38.84	24.07	6.27
29	627.2	35.30	21.88	5.93
30	603.2	19.21	11.91	3.36

Table 3. Correlation between device readings and physical-mechanical properties of flax fiber.

Quality indicator	Correlation coefficient (R)
Linear density	0.95
Flexibility	–0.68
Breaking load	0.68
Color group	–0.20

RESULTS AND DISCUSSION

During the analysis of flax fiber, the developed device was used for rapid quality assessment by measuring its sound-absorbing properties. Based on the obtained results, the fiber can be objectively characterized in terms of flexibility, linear density, and breaking load. To identify the relationship between the device readings and fiber quality parameters—linear density, breaking load, flexibility, and color group—a correlation analysis was performed using the described methodology. MS Excel was used for the analysis.

Table 4 presents the data used to determine the relationship between the fiber's sound-absorbing properties, as measured by the developed device, and its linear density, flexibility, breaking load, and color group.

To establish the relationship between the sound absorption properties of flax fiber and its physical and mechanical characteristics, measurements of 30 fiber samples were carried out on the developed device with tenfold repetition according to the above recommendations. To determine the dependence of the instrument readings on quality indicators such as linear density, breaking load, flexibility, and color group, a correlation analysis was conducted between the fiber quality parameters and the instrument readings. Based on this analysis, correlation coefficients were calculated and the following equations were obtained (1), (2), (3).

Relationship between the device readings x_1 and the linear density of flax fiber y_1:

$$y_1 = 0.9487\, x_1^{0.365} \quad (1)$$

Relationship between the device readings x_1 and the flexibility of flax fiber y_2:

$$y_2 = 208\, x_1^{-0.269} \quad (2)$$

Relationship between the device readings x_1 and the breaking load of flax fiber y_3:

$$y_3 = 8.3932 \ln(x_1) - 29.05 \quad (3)$$

The Figure 10 below shows a graphical representation of this relationship as an example.

The results of statistical processing and correlation analysis indicate a significant correlation at the 0.05 significance level between the device readings and all tested quality indicators of flax fiber, except for the color group, which shows no correlation, as evidenced by a correlation coefficient of 0.20.

Table 4. Source data for determining the relationship between the device readings and the physico-mechanical quality parameters of the fiber.

Batch number	Device readings, relative units	Quality indicators			
		Linear density, tex	Breaking load, daN	Flexibility, mm	Color group
	y_1	x_1	x_2	x_3	x_4
1	1324.6	12.5	29.2	42.7	2.2
2	550.8	10.0	26.8	43.5	1.7
3	1250.2	13.0	32.3	42.8	2.9
4	1203.4	12.5	29.3	37.4	3.0
5	1148.5	12.7	31.7	41.9	2.2
6	957.4	10.9	26.4	43.1	2.2
7	747.5	10.7	28.2	43.1	3.0
8	1121.3	12.5	31.5	38.7	2.4
9	1577.4	13.7	29.7	34.8	1.9
10	773.7	11.3	37.4	46.5	3.2
11	1982.6	14.7	32.0	40.5	3.0
12	204.4	7.1	22.2	65.6	2.6
13	435.3	8.9	24.5	49.0	3.1
14	902.4	11.0	24.6	45.2	3.0
15	754.8	10.2	20.1	51.9	1.8
16	1343.0	13.5	33.1	41.4	1.9
17	985.3	11.9	27.4	49.0	1.8
18	3876.6	19.8	40.3	32.5	1.9
19	1533.0	14.4	32.6	40.3	2.3
20	677.7	10.4	27.6	50.1	2.1
21	422.7	8.9	24.4	54.3	2.9
22	253.3	7.2	15.2	70.0	3.0
23	554.8	9.7	21.6	50.3	2.2
24	450.9	8.9	24.3	54.2	2.4
25	181.5	6.0	5.0	82.1	2.9
26	391.9	7.9	18.4	55.8	2.8
27	552.4	9.0	24.7	46.9	1.5
28	652.5	9.4	25.5	50.2	2.0
29	627.2	9.6	33.4	50.1	2.8
30	603.2	10.3	17.1	47.0	1.5

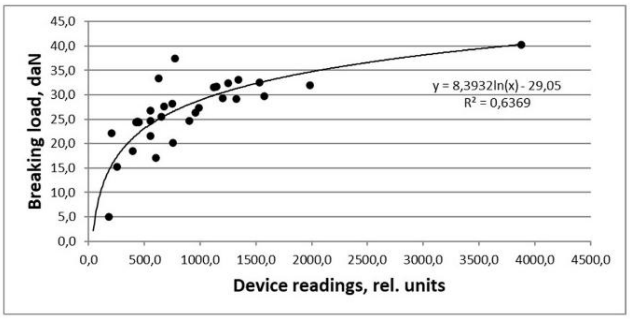

Figure 10. Relationship between instrument readings and the breaking load of flax fiber.

To test for differences in the mean values of samples obtained by measuring flax fiber quality indicators using the standard method according to DSTU 4015-2001 and calculated using the proposed formulas, the Student's t-test was applied. Analysis of the flax fiber quality indicators determined using the standard methods (DSTU 4015-2001 and GOST 10878-70) and those calculated by the proposed methods with the device showed a high degree of agreement. The empirical Student's *t*-test values for linear density, flexibility, breaking load, and color group were significantly lower than the critical value ($t_{critical}$ = 2.05) at a 0.95 significance level, allowing the null hypothesis (H_0) of no significant difference between measurement results to be accepted with 95% confidence. Furthermore, high correlation coefficients (ranging from 0.80 to 0.99) confirm a strong positive relationship between the standard methods and the proposed approaches. Thus, the developed methods provide reliable assessment of the physical and mechanical properties of flax fiber, accurately reflecting the trends established by standard methods.

Thus, when using the device, the fiber sample mass should be 10 g, the operating frequency of the device set at 1750 Hz, the height of the measurement chamber 48 mm, and the measurements must be performed with tenfold repetition.

The reproducibility and accuracy of the proposed sensory method must be evaluated against existing instrumental standards, as precision alone does not guarantee compliance with measurement correctness. Therefore, both accuracy and precision should be monitored and maintained over time. To assess measurement stability, Shewhart control charts were used, serving as a diagnostic tool to identify sources of variability in the measurement process. For this purpose, a random batch of flax fiber was selected, from which twenty samples were taken and measured.

The measurement uncertainty was evaluated as follows: over four days, flax fiber from a single batch was measured using the proposed device, with eight

measurements taken each day. The calculated Fisher criterion was F_{emp}=1.04, while the critical value for a 0.95 confidence level with 3 and 28 degrees of freedom was F_{tab}=2.95. Since $F_{emp} < F_{tab}$, the data homogeneity is satisfactory. The estimated variance was S^2=184.2, giving an expanded measurement uncertainty of U=58.4. The relative error at a 0.95 confidence level was 1.99%, the confidence interval ±24.8, and the relative expanded uncertainty 4.7%. Therefore, the measurement result is 1245.7±24.8, which is acceptable, as the error is below 5%.

Thus, the developed methods for determining the quality indicators of flax fiber are consistent with the evaluation levels established by standard methods, as confirmed by the Student's *t*-test, and demonstrate the same evaluation trends, as evidenced by the significance of the correlation coefficients.

The analysis of the obtained results indicates that, at a statistical significance level of 0.05, there is a certain correlation between the fiber number and the readings obtained using the described method and device. Specifically, a significant direct relationship was established between the fiber number N (according to the State Standard of Ukraine) and the instrument readings characterizing the acoustic sound absorption properties of the fiber, as confirmed by the correlation coefficient r_3 = 0.65.

According to the analysis results, the sound absorption coefficient was determined, which can be expressed by the following equation:

$$K=1.005\text{-}8 \cdot 10\text{-}6 \cdot r_3 \quad (4)$$

This coefficient is applied in the derived empirical formula, which makes it possible to calculate the fiber number by taking into account the measurement results of the light-reflecting, light-absorbing, and sound-absorbing properties of flax fiber, as demonstrated in our research. The relevance of the developments is confirmed by the obtained Patent of Ukraine No. 47840.

To verify the validity of Equation (4), additional analysis was carried out by comparing the acoustic response measured using the developed device with the sound-absorbing properties of flax fiber samples characterized by independent physical-mechanical parameters. The analysis was performed on 30 samples with ten repeated measurements for each sample. The obtained statistically significant correlations confirm that the proposed acoustic measurement approach adequately reflects the sound-absorbing behavior of the fibrous material.

To validate Equation (4), an experimental study was carried out using a dataset of 30 samples of scutched flax fiber with different physical and mechanical properties. For each sample, the following parameters were measured: fiber length L, acoustic response of the fibrous layer ZP obtained using the developed acoustic device. The reference quality parameter was the fiber number determined according to DSTU 4015-2001.

Statistical analysis of the experimental data showed that the average fiber number was 12.6 (range 8–15), the average fiber length was 64.6 (41–88.6) and the average acoustic response was 934.7 relative units (181.5–3876.6).

To determine the significance of the factors, pair correlation coefficients between the fiber number and the measured parameters were calculated. The strongest correlation was observed for fiber length (r=0.93), while acoustic response also showed significant positive correlations with fiber quality (r=0.65). Finally, the coefficient K describing the acoustic properties of the fibrous layer was obtained (Equation 4).

The results demonstrate that the acoustic response parameter shows a statistically significant correlation with the standardized fiber quality indicator (r=0.65). This confirms that the acoustic measurement approach used in the developed device can serve as an informative indirect indicator of flax fiber quality and supports the validity of the empirical relationship expressed in Equation (4).

The presented research introduces a novel, non-destructive acoustic method for the rapid quality assessment of flax fiber by measuring its sound absorption properties. The study successfully established a measurable link between the device's readings and critical quality indicators like linear density, breaking load, and flexibility. This acoustic approach offers a significant advantage in speed and efficiency compared to conventional, time-consuming testing methods, directly addressing the industry need for better real-time quality control.

While the methodology successfully defined optimal operating parameters — a 10 g sample mass, a 1750 Hz operating frequency, and a critical 12% moisture content — a closer look reveals areas for discussion. The dependence on a precisely controlled moisture level (12% reference) suggests a practical limitation; any deviation in ambient humidity or fiber storage conditions could necessitate pre-conditioning, partially undermining the "rapid" nature of the test.

Furthermore, the strong statistical validation using the Student's t-test and high correlation coefficients (ranging from 0.80 to 0.99) is compelling evidence that the method reflects the trends of standard methods. However, the mechanism of correlation, particularly the inverse relationship with flexibility (Equation (2)), warrants deeper physical modeling. The current analysis attributes sound absorption to bulk density and structural properties. Future work should investigate the role of fiber fineness distribution and the porosity/tortuosity of the packed sample more directly, as these microstructural factors fundamentally govern acoustic energy dissipation in fibrous media.

A key limitation is the device's reliance on a packed fiber sample (10 g within a fixed volume). This packed state creates an artificial acoustic medium whose properties are influenced by how the sample is prepared (e.g., initial packing pressure or fiber orientation). This could introduce a source of variability not fully captured by the current uncertainty analysis, despite the tenfold repetition.

The successful derivation of an empirical formula and the determination of the sound absorption coefficient *K* (Equation (4)) are crucial for standardizing the new method. Ultimately, the relevance of this patented device will depend on its ability to transition from a laboratory tool to a robust, low-maintenance instrument capable of consistently and economically outperforming the existing standard tests in industrial settings, which remains the final benchmark for true innovation in fiber quality assessment.

CONCLUSIONS

This research successfully demonstrated and validated a novel, non-destructive method for the rapid determination of key quality indicators of flax fiber utilizing the principle of sound absorption. Through the development and rigorous optimization of a new measuring device, critical operational parameters essential for ensuring the accuracy and repeatability of results were established. The optimal settings for objective fiber quality assessment were determined to be a 10 g sample mass, an emitter operating frequency of 1750 Hz (corresponding to the required chamber length of $\lambda/4$), and a reference fiber moisture content of 12%. The most significant outcome is the discovery of a strong statistical correlation between the instrument readings, which reflect the acoustic properties of the sample, and the main physical and mechanical characteristics of the fiber. Specifically, a direct and significant relationship was established with linear density and breaking load, alongside an inverse relationship with flexibility. This confirms that the acoustic response of the packed fiber is a reliable indicator of its structural integrity and mechanical performance. The high degree of agreement between the results obtained using the developed device and those determined by standard methods (DSTU 4015-2001) was confirmed by the Student's *t*-test, which showed no statistically significant difference between the mean values. This, coupled with high correlation coefficients (up to 0.99), strongly validates the reliability and reproducibility of the proposed methodology. Furthermore, empirical formulas were derived, allowing for the direct calculation of quality indicators from the acoustic measurements. This, along with the acceptable estimation of expanded measurement uncertainty (relative error below 5 %), positions the developed method as a reliable and precise tool for industrial quality control. Beyond the development of the quality assessment tool, this research established the foundation for practical, high-value applications by formulating the conceptual diagram of the active robotic noise-mitigation panel based on flax fiber. This conceptualization integrates the passive acoustic absorption properties of flax with a dynamic control system utilizing real-time sensor feedback and actuation elements. This innovative framework is designed to enable the fiber's use in advanced robotic landscaping systems for autonomous noise control in urban and public environments. The need to accurately and rapidly assess the quality and acoustic potential of the flax fiber core for this active panel directly motivated the development of the sound-absorption based testing method presented herein. In conclusion, the developed acoustic method constitutes a viable, rapid, and non-destructive alternative for quality control in flax fiber processing. Crucially, the integration of this reliable material assessment capability supports the advancement of sustainable materials into the domain of smart, active noise control technologies, providing the industry with efficient means for both objective material evaluation and innovative product development.

REFERENCES

1. Tolmachov V., Riabko A.: Use of arduino-compatible systems in devices for determination of color indicators of flax fiber, Vlakna a Textil, 29(4), 2023, pp. 45-60. https://doi.org/10.15240/tul/008/2022-4-006
2. Bi Z., Li Q., Zhang Z., et al.: Experimental and numerical evaluation of the influence of voids on sound absorption behaviors of 3D printed continuous flax fiber reinforced PLA composites, Composites Science and Technology, 2024 110720 P. https://doi.org/10.1016/j.compscitech.2024.110720
3. Sathesh Babu M., Ramamoorthi R., Gokulkumar S., et al.: Mahua oil cake microcellulose as a performance enhancer in flax fiber composites: mechanical strength and sound absorption analysis, Polymer Composites, 2024, pp. 1-20. https://doi.org/10.1002/pc.29100
4. Periyasamy D., Manoharan B., Arockiasamy F.S., et al.: Exploring the recycling potential of HDPE films reinforced with flax fiber for making sustainable decorative tiles, Journal of Materials Research and Technology, 25, 2023, pp. 2049-2060. https://doi.org/10.1016/j.jmrt.2023.06.067
5. Bhuvaneswari V., Devarajan B., Arulmurugan B., et al.: A critical review on hygrothermal and sound absorption behavior of natural-fiber-reinforced polymer composites, Polymers, 14(21), 2022, 4727 P. https://doi.org/10.3390/polym14214727
6. Haris A., Kureemun U., Tran L.Q.N., et al.: Water uptake and its effects on mechanical and acoustic properties of flax/polypropylene composite, Journal of Natural Fibers, 18(9), 2021, pp. 1344-1358. https://doi.org/10.1080/15440478.2019.1691112
7. Gliscinska E., Perez de Amezaga J., Michalak M., et al.: Green sound-absorbing composite materials of various structure and profiling, Coatings, 11(4), 2021, 407 P. https://doi.org/10.3390/coatings11040407
8. Mohammadi M., Taban E., Tan W.H., et al.: Recent progress in natural fiber reinforced composite as sound absorber material, Journal of Building Engineering, 2024, 108514 P. https://doi.org/10.1016/j.jobe.2024.108514
9. Kudva A., Gt M., Pai K.D.: Physical, thermal, mechanical, sound absorption and vibration damping characteristics of natural fiber reinforced composites and hybrid fiber reinforced composites: A review, Cogent Engineering, 9(1), 2022, 2107770 P. https://doi.org/10.1080/23311916.2022.2107770

10. Madushika J.W.A., Lanarolle W.D.G.: A review on novel approaches to enhance sound absorbing performance using textile fibers, The Journal of The Textile Institute, 113(2), 2022, pp. 341-348. https://doi.org/10.1080/00405000.2021.1872831
11. Gumanová V., Sobotová L., Dzuro T., et al.: Experimental survey of the sound absorption performance of natural fibres in comparison with conventional insulating materials, Sustainability, 14(7), 2022, 4258 P. https://doi.org/10.3390/su14074258
12. Su J., Yang X., Yao Y., et al.: Advanced three-dimensional textile technique for fabrication of sisal/flax hybrid fiber green biocomposite with enhanced mechanical, thermal, and sound isolation properties, Industrial Crops and Products, 223, 2025, 120174 P. https://doi.org/10.1016/j.indcrop.2024.120174
13. Rotini F., Fiorineschi L., Conti L., et al.: Investigating Polylactic Acid Foam–Plant Fiber Composites for Sound Absorption and Insulation, Sustainability, 16(16), 2024, 6913 P. https://doi.org/10.3390/su16166913
14. Liang M., Wu H., Liu J., et al.: Improved sound absorption performance of synthetic fiber materials for industrial noise reduction: A review, Journal of Porous Materials, 29(3), 2022, pp. 869-892. https://doi.org/10.1007/s10934-022-01219-z
15. Jang E.S.: Sound absorbing properties of selected green material. A review, Forests, 14(7), 2023, 1366 P. https://doi.org/10.3390/f14071366
16. Sleinus D., Sinka M., Korjakins A., et al.: Properties of sound absorption composite materials developed using flax fiber, sphagnum moss, vermiculite, and sapropel. Materials, 16(3), 2023, 1060 P. https://doi.org/10.3390/ma16031060
17. Yang T., Hu L., Xiong X., et al.: Sound absorption properties of natural fibers: A review. Sustainability, 12(20), 2020, 8477 P. https://doi.org/10.3390/su12208477

AIMS AND SCOPES

“Vlakna a Textil” is a peer-reviewed scientific journal serving the fields of fibers, textile structures and fiber-based products including research, production, processing, and applications.

The birth of this journal is connected with three institutions, Research Institute for Man-Made Fibers, Svit (VÚCHV), Research Institute of Chemistry of Textiles (VÚTCH) in Žilina and Department of Fibers and Textiles at the Faculty of Chemical Technology, Slovak Technical University in Bratislava, having a joint intention to provide, utilize and deposit results obtained through the research, development and production activities dealing with the aforementioned scopes. „Vlákna a Textil“ journal has been launched as a consequence of a joing of existing magazines „Chemické vládkna“ (VÚCHV) and „Textil a chémia“ (VÚTCH). Their tradition should provide a good framework for the new journal with the main aim to create a closer link between the basic element of the product - fibre and its fabric - textile.

Since its founding in 1994, the journal introduces new concepts, innovative technologies and better understanding of textile materials (physics and chemistry of fiber forming polymers), processes (technological, chemical and finishing), garment technology and its evaluation (analysis, testing and quality control) including non-traditional applications, such as technical textiles, composites, smart textiles or garment, and nano applications among others. The journal publishes original research papers and reviews. Original papers should present a significant advance in the understanding or application of materials and/or textile structures made of them.

VLÁKNA A TEXTIL
Volume 33, Issue 1, April 2026

CONTENT